Sedimentology and provenance of the Upper Jurassic Naknek Formation, Talkeetna Mountains, Alaska: Bearings on the accretionary tectonic history of the Wrangellia composite terrane

Jeffrey M. Trop[†]
Darren A. Szuch[‡]
Department of Geology, Bucknell University, Lewisburg, Pennsylvania 17837, USA

Matthew Rioux[§]
Department of Geological Sciences, University of California, Santa Barbara, California 93106, USA

Robert B. Blodgett[#]
U.S. Geological Survey, 4200 University Drive, Anchorage, Alaska 99508, USA

ABSTRACT

Analysis of the Upper Jurassic Naknek Formation in the Talkeetna Mountains, Alaska, documents synorogenic sedimentation in a forearc basin along the outboard (southern) margin of the allochthonous Peninsular terrane during accretion to the western North American continental margin. New geochronologic, sedimentologic, and compositional data define a two-part stratigraphy for the Naknek Formation. Microfossil, megafossil, and U-Pb clast ages document early Oxfordian to early Kimmeridgian deposition of the lower 690 m of the Naknek Formation and early Kimmeridgian to early Tithonian deposition of the upper 225 m of the Naknek Formation. Lithofacies and paleocurrent data from the lower Naknek Formation demonstrate initial deposition on a high-gradient, southward-dipping basin floor. Submarine mass flows deposited poorly sorted, cobble-boulder conglomerate in proximal fan-delta environments. Gravelly mass flows transformed downslope into sandy turbidity currents on a muddy prodelta slope. During early Kimmeridgian to early Tithonian time, fan-delta environments were replaced by lower gradient marine shelf environments characterized by deposition of cross-stratified sandstone and bioturbated mudstone. Source-diagnostic clasts, feldspathic sandstone compositions, southward-directed paleocurrent indicators, and U-Pb zircon ages of plutonic clasts (167.6 ± 0.3 Ma; 166.5 ± 0.2 Ma, 164–159 Ma, 156.2 ± 0.4 Ma) indicate that the Naknek Formation was derived primarily from volcanic and plutonic source terranes exposed along the northern basin margin in the southern Talkeetna Mountains. Geologic mapping documents the Little Oshetna fault, a newly identified northward-dipping reverse fault that bounds the northern margin of the Naknek Formation in the Talkeetna Mountains. The concentration of boulder-rich mass-flow deposits in the footwall of the fault in combination with geochronologic and compositional data suggest that sedimentation was coeval with Late Jurassic shortening along the fault and exhumation of plutonic source terranes exposed in the hanging wall of the fault. From a regional perspective, coarse-grained forearc sedimentation and pluton exhumation along the outboard (southern) segment of the Peninsular terrane were coeval with crustal-scale shortening and synorogenic sedimentation in retroarc basins along the inboard (northern) margin of the Wrangellia terrane (Kahiltna, Nutzotin, and Wrangell Mountains basins). We interpret the regional and synchronous nature of Late Jurassic crustal-scale deformation and synorogenic sedimentation in south-central Alaska as reflecting either initial collision of the Wrangellia and Peninsular terranes with the former continental margin of western North America or amalgamation of the two terranes prior to collision.

Keywords: Alaska, forearc basin, Naknek Formation, Peninsular terrane, sedimentology, Wrangellia terrane.

INTRODUCTION

The Late Jurassic–Early Cretaceous tectonic evolution of southern Alaska is critical to the ongoing debate concerning the accretionary development of the western North American Cordillera (e.g., Cowan et al., 1997). The Wrangellia composite terrane, one of the largest accreted terranes in the Cordillera, consists of three tectonostratigraphic terranes: the Peninsular, Wrangellia, and Alexander terranes (PT, WT, AT in Fig. 1A; Plafker and Berg, 1994). The Alexander and Wrangellia terranes were joined together by middle Pennsylvanian time (Gardner et al., 1988), positioned ~20–30° south of their present latitude during Late Triassic time (Plafker et al., 1989; Hillhouse and Coe, 1994), and translated northward to moderate paleolatitudes by latest Cretaceous time before Eocene arrival in Alaska (Hillhouse and Coe, 1994; Stamatakos et al., 2001). The Peninsular terrane was juxtaposed against the combined Alexander-Wrangellia terrane sometime between Permian and Cretaceous time, but unequivocal cross-cutting relationships with the adjacent Wrangellia terrane have not been reported. Moreover, the precise timing, nature, and location of initial accretion of the Wrangellia composite terrane

[†]E-mail: jtrop@bucknell.edu.
[‡]Present address: Blasland, Bouck, and Lee, Inc., 8 South River Road, Cranbury, New Jersey 08512, USA; e-mail: dszuch@bbl-inc.com.
[§]E-mail: mrioux@umail.ucsb.edu.
[#]E-mail: rblodgett@usgs.gov.

GSA Bulletin; May/June 2005; v. 117; no. 5/6; p. 570–588; doi: 10.1130/B25575.1; 11 figures; 2 tables; Data Repository item 2005077.

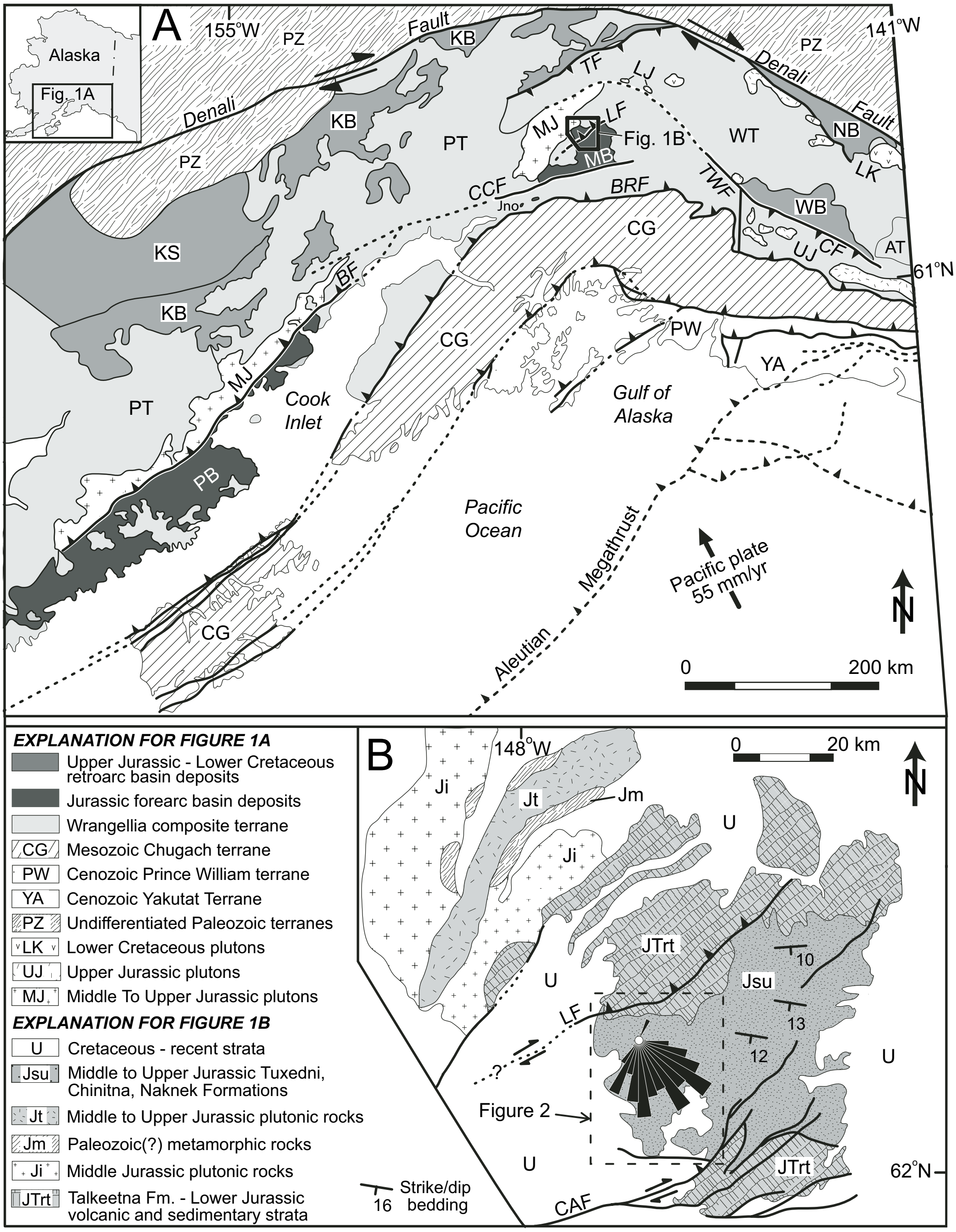

Figure 1. (A) Map showing terranes, Mesozoic sedimentary basins, and Mesozoic magmatic arcs of southern Alaska. Tectonostratigraphic terranes: PT—Peninsular; WT—Wrangellia; AT—Alexander; PZ—undifferentiated, mostly Paleozoic metamorphic rocks of the Yukon Tanana terrane. Jurassic-Cretaceous basins: NB—Nutzotin; WB—Wrangell Mountains; MB—Matanuska Valley–Talkeetna Mountains; PB—Alaska Peninsula; KB—Kahiltna. Cretaceous basin: KS—Kuskokwim. Fault systems: CCF—Castle Mountain–Caribou; BF—Bruin Bay; LF—Little Oshetna; TF—Talkeetna; CF—Chitina; BRF—Border Ranges; TWF—Taral–West Fork. Adapted from Nokleberg et al. (1994) and Plafker et al. (1994). Jno—small outliers of Upper Jurassic Naknek Formation in western Chugach Mountains. Black polygon shows area of Figure 1B. Inset is a smaller-scale political map of the region. (B) Geologic map of the southeastern Talkeetna Mountains. LF—Little Oshetna fault; CAF—Caribou strand of the Castle Mountain fault system. Rose diagram represents structurally restored paleocurrent data (n = 207) from the Upper Jurassic Naknek Formation. Paleocurrent data include unidirectional indicators (n = 198; clast imbrication, planar cross-stratification) and sparse bidirectional indicators (n = 9; groove casts). See Szuch (2002) for raw paleocurrent data. Geology modified from Wilson et al. (1998) and Csejtey et al. (1978).

with the continental margin of western North America are controversial (e.g., McClelland et al., 1992; Plafker and Berg, 1994; Cowan et al., 1997). Numerous tectonic models postulate initial late Early to early Late Cretaceous collision based on regional shortening, synorogenic plutonism, and metamorphism along the inboard margin (northeastern, present coordinates) of the composite terrane (e.g., Csejtey et al., 1982; Monger et al., 1982; Nokleberg et al., 1985; Crawford et al., 1987; Rubin and Saleeby, 1992). Other studies propose Middle Jurassic–Early Cretaceous collision based on regional pre–Late Cretaceous deformation and sedimentation (e.g., McClelland and Gehrels, 1990; McClelland et al., 1992; van der Heyden, 1992; Kapp and Gehrels, 1998; Gehrels, 2001; Trop et al., 2002; Ridgway et al., 2002). If pre-Cretaceous accretionary tectonics influenced the Wrangellia composite terrane, existing tectonic models may underestimate the duration and amount of crustal shortening within the accreted terranes. Moreover, understanding relationships between terrane accretion and inboard tectonic events (i.e., Nevadan and Sevier orogenies) along the former western continental margin of North America requires improved constraint on the paleogeographic history of the Wrangellia composite terrane.

Mesozoic sedimentary strata exposed in southern Alaska provide a valuable record of basin formation, deformation, and exhumation within the Wrangellia composite terrane. Upper Jurassic to Upper Cretaceous sedimentary strata are regionally exposed between the composite terrane and the Mesozoic continental margin of North America and have estimated thicknesses of 3–10 km (NB, KB, KS, WB in Fig. 1A). The position of these strata inboard (northward, present coordinates) of Middle to Upper Jurassic plutons (MJ-LJ in Fig. 1A) and a Mesozoic accretionary prism (CG in Fig. 1A) indicate deposition in retroarc basins along a northward-dipping subduction zone (present coordinates; Plafker and Berg, 1994). Sedimentologic, compositional, and structural data from the retroarc basin deposits document Late Jurassic–Early Cretaceous contractile shortening, exhumation, and synorogenic sedimentation attributable to collision of the Wrangellia composite terrane (e.g., Trop et al., 2002; Ridgway et al., 2002; Manuszak, 2000). Jurassic-Cretaceous sedimentary strata are also preserved in a forearc position (MB, PB in Fig. 1A) between the Middle to Upper Jurassic plutons and Mesozoic accretionary prism. However, published studies of the thick, laterally extensive forearc basin deposits in the Talkeetna Mountains (MB in Fig. 1A; Jsu in Fig. 1B) are limited to geologic mapping (Grantz, 1960a, 1960b) and megafossil studies (Imlay, 1981; Imlay and Detterman, 1973). This paper presents new geochronologic, biostratigraphic, sedimentologic, and compositional data needed to characterize the age, deposystems, provenance, and tectonic framework of Upper Jurassic forearc basin deposits. Our results permit integrative analysis of collisional forearc and retroarc basin development, document stratigraphic linkages between the Peninsular and Wrangellia terranes, and provide a potential piercing point for postcollisional strike-slip displacement along the Castle Mountain fault, which bisects the forearc basin.

GEOLOGIC SETTING

Middle to Upper Jurassic sedimentary strata are part of a 45-km-long outcrop belt north of the Castle Mountain fault system in the Talkeetna Mountains (MB in Fig. 1A; Wilson et al., 1998) and a 1150-km-long outcrop belt south of the fault system along the Alaska Peninsula (PB in Fig. 1A; Detterman et al., 1996). Two isolated outcrops of Upper Jurassic strata are also exposed south of the Castle Mountain fault system in the northern Chugach Mountains (Jno in Fig. 1A; Barnes, 1962; Pavlis et al., 1988). Sedimentary strata were deposited in a forearc basin that formed between a coeval batholith to the north in the Talkeetna Mountains and Alaska Peninsula (MJ in Fig. 1A) and an accretionary prism to the south in the Chugach Mountains (CG in Fig. 1A; Plafker and Berg, 1994). The accretionary prism consists of metamorphosed Triassic-Paleogene marine strata and mélange that locally have Early to Late Jurassic depositional and metamorphic ages (Plafker et al., 1989, 1994; Roeske et al., 1989). Within the accretionary prism, the age of deposits, degree of structural deformation, and grade of metamorphism decrease southward, indicating persistent northward-directed subduction (present coordinates; Plafker et al., 1989, 1994). The batholith consists mainly of felsic plutons that have Middle to early Late Jurassic crystallization ages (177–156 Ma; Rioux et al., 2002, 2003). The plutons locally intrude the Talkeetna Formation, a 3,000-m-thick sequence of lava flows, volcaniclastic rocks, and minor sedimentary strata that represent the volcanic edifice of an Early Jurassic intraoceanic island arc (Talkeetna arc; Barker and Grantz, 1982; Nokleberg et al., 1994). The Talkeetna Formation and Jurassic plutons represent the upper structural levels of the allochthonous Peninsular terrane (PT in Fig. 1A).

The Mesozoic forearc-basin stratigraphy of the Talkeetna Mountains consists of unconformity-bound sequences that are dominated by marine siliciclastic strata. The Middle Jurassic Tuxedni (Bajocian-Bathonian) and Chinitna (Bathonian-Callovian) Formations overlie volcanic and sedimentary strata of the Lower Jurassic Talkeetna Formation along an angular unconformity. The Tuxedni and Chinitna Formations consist mainly of mudstone and fine-grained sandstone deposited in shallow marine deposystems (Grantz, 1960a, 1960b; Winkler, 1992). The Upper Jurassic (Oxfordian-Kimmeridgian) Naknek Formation, the focus of this study, disconformably overlies the Chinitna Formation and consists of a coarse-grained sequence of marine conglomerate, sandstone, and mudstone (Grantz, 1960a, 1960b; Imlay and Detterman, 1973; Imlay, 1981). The Lower Cretaceous (Valanginian-Hauterivian) Nelchina Limestone, Upper Cretaceous (Albian-Maastrichtian) Matanuska Formation, and unnamed Paleogene sedimentary and volcanic rocks unconformably overlie the Naknek Formation (Grantz, 1960a, 1960b; Jones, 1964, 1967; Trop et al., 2003; Cole, 2003).

The northern and southern margins of the Jurassic forearc basin strata are bound by the Little Oshetna and Castle Mountain faults, respectively (Fig. 2). The Little Oshetna fault, a previously unreported thrust fault, strikes northeast-southwest and dips northwest ~55° (Fig. 2). The minimum amount of reverse displacement across the fault is ~550 m based on the juxtaposition of the lower Talkeetna Formation in the hanging wall against the uppermost Talkeetna Formation and overlying Middle to Upper Jurassic sedimentary strata in the footwall (Fig. 2). A substantially larger estimate of vertical displacement is permissible given the 3,000+ m maximum thickness of the Talkeetna Formation. Possible horizontal displacement along the fault is presently not constrained. The Billy Mountain fault, a northern strand of the Castle Mountain fault system, bounds the southern margin of the study area (Fig. 2). Offset Tertiary geologic features and low-angle slickenlines along the fault zone indicate strike-slip displacement. Tens of kilometers of Cretaceous-Tertiary dextral strike-slip displacement characterize other segments of the Castle Mountain fault system (e.g., Grantz, 1966; Clardy, 1974; Fuchs, 1980).

LATE JURASSIC SEDIMENTATION

The Upper Jurassic Naknek Formation, the focus of this study, is divided into two informal members that include three mappable lithofacies associations (Figs. 2–5; Grantz, 1960a, 1960b). The lower Naknek Formation has a maximum preserved thickness of ~690 m and comprises a conglomeratic fan-delta lithofacies association (Jn1) and a laterally equivalent prodelta lithofacies association (Jn2). The upper

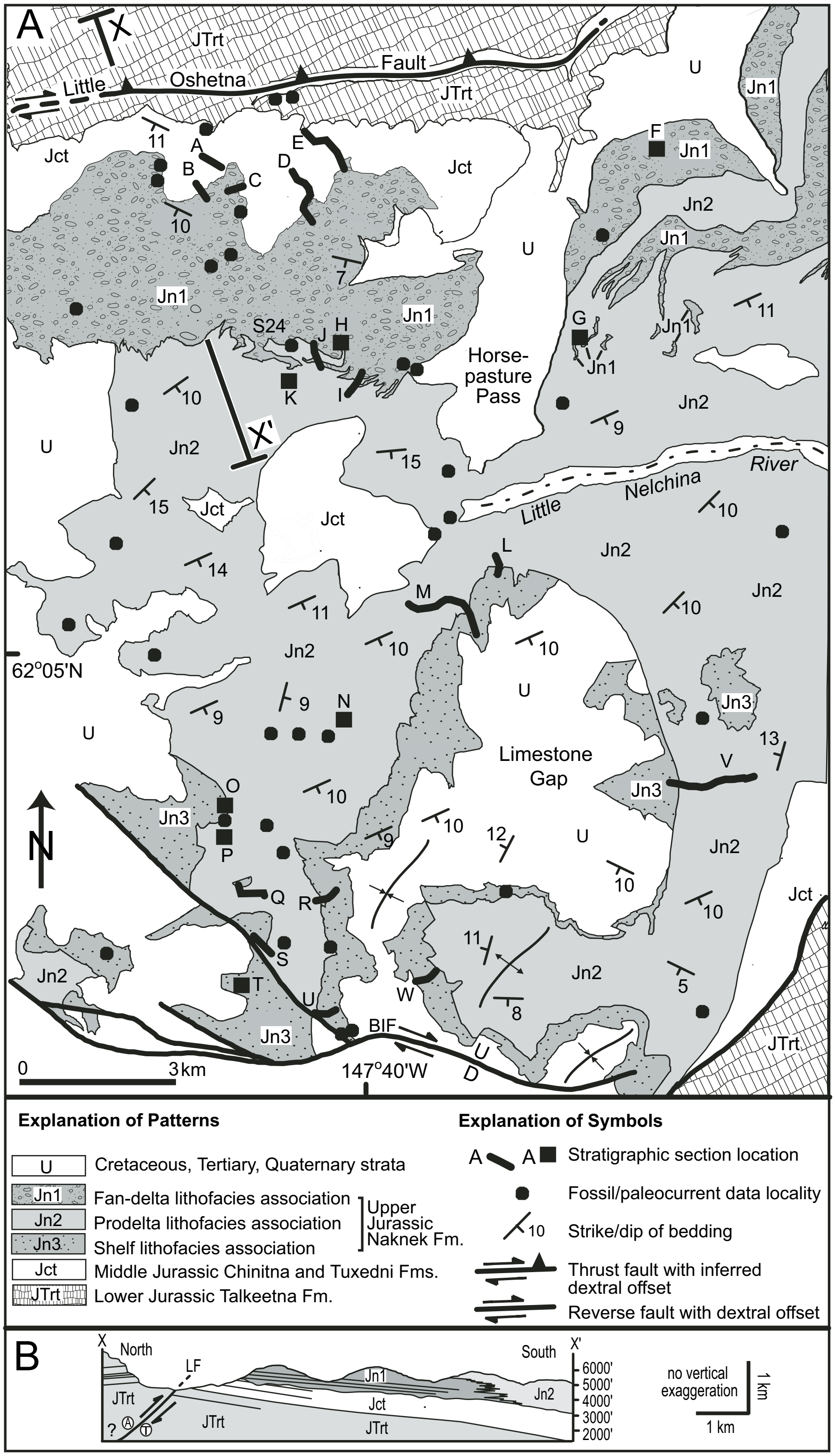

Figure 2. (A) Geologic map of the southeastern Talkeetna Mountains showing Naknek Formation lithofacies associations, major faults, and locations of measured sections. Our aerial reconnaissance and mapping indicate that this map area includes the most extensive, well-exposed outcrops of the Naknek Formation in the Talkeetna Mountains, although similar lithofacies associations extend laterally to the northeast for ~30 km. Geology modified from Grantz (1960a). (B) Geologic cross section showing faulted northern margin of the Naknek Formation outcrop belt. Data used to construct cross section from this study and Grantz (1960a).

Naknek Formation has a maximum preserved thickness of ~225 m and comprises a shallow marine shelf lithofacies association (Jn3). New biostratigraphic, geochronologic, sedimentologic, and compositional data presented in the following sections permit reconstruction of forearc basin deposystems and source terranes during Late Jurassic sedimentation.

Biostratigraphic and Geochronologic Data

The age of the Naknek Formation in the Talkeetna Mountains was previously interpreted as early Oxfordian to early Tithonian (Late Jurassic) based on marine megafossils collected within the context of regional mapping studies (Imlay and Detterman, 1973; Imlay, 1981). New biostratigraphic and geochronologic data collected within the context of measured stratigraphic sections set limits on the age range of individual lithofacies associations (Figs. 3–5). Age data and methods are presented in Table 1 and Tables DR1–3.[1] Our new age data demonstrate early Oxfordian to early Kimmeridgian (ca. 159–152 Ma; Fig. 3) deposition of the lower Naknek Formation (Jn1, Jn2 in Figs. 4 and 5). Oxfordian foraminifera and radiolaria microfossils were obtained from samples spanning ~600 m of the lower Naknek Formation (Fig. 5; Table DR1; M. Mickey and S. Kling, personal commun., 2001). A middle to late Oxfordian ammonite was also collected from the lower Naknek Formation (*Phylloceras iniskinense*; Fig. 5; Fig. DR1), consistent with previously reported early to late Oxfordian ammonites from the Naknek Formation (Fig. 3; Imlay, 1981). *Buchia concentrica* bivalves in the upper part of the lower Naknek Formation indicate that deposition continued through late Oxfordian to early Kimmeridgian time (Fig. 5; Fig. DR1A–1C). U-Pb zircon analyses of igneous clasts from lower Naknek Formation conglomerate beds provide crude maximum ages of deposition that support the biostratigraphic data. Chemical abrasion analysis of zircons from three plutonic clasts yielded pre-Oxfordian ages (Figs. 3 and 6; 167.6 ± 0.3 Ma; 166.5 ± 0.2 Ma; 164–159 Ma). An early Kimmeridgian to early Tithonian (ca. 152–148 Ma) depositional age is inferred for the upper Naknek Formation (Jn3 in Figs. 4 and 5) based on the presence of *Buchia mosquensi* bivalves (Table DR2; Fig. 5; Fig. DR1). This biostratigraphic interpretation is supported by an Oxfordian U-Pb zircon age (156.2 ± 0.4 Ma) from a plutonic clast contained in an upper Naknek Formation conglomerate bed

[1]GSA Data Repository item 2005077, Figure DR1 and Tables DR1–4, is available on the Web at http://www.geosociety.org/pubs/ft2005.htm. Requests may also be sent to editing@geosociety.org.

(Figs. 3 and 6). In summary, the lower 690 m of the Naknek Formation was deposited during early Oxfordian to early Kimmeridgian time, whereas the upper 225 m of the Naknek Formation was deposited during early Kimmeridgian to early Tithonian time.

Sedimentological Data

The Naknek Formation in the Talkeetna Mountains consists of conglomerate, sandstone, mudstone, and limestone as much as 915 m thick. Facies analyses, paleocurrent determinations, and particle size data were obtained within the context of 23 bed-by-bed measured stratigraphic sections and 28 isolated outcrops (Fig. 2). Representative measured sections are shown in Figure 5. Paleocurrent indicators were measured from 26 beds at 12 different locations, totaling 207 measurements (Fig. 1B). Particle size data were collected from 126 conglomerate beds at 17 locations, totaling 930 measurements (Figs. 4 and 5). The excellent lateral continuity of outcrops and lack of intense structural deformation permitted two-dimensional observations of depositional architecture and facies associations over hundreds of meters to several kilometers. Collectively, these data characterize three lithofacies associations: fan delta, prodelta, and marine shelf. In the following section, each facies association is briefly described and interpreted.

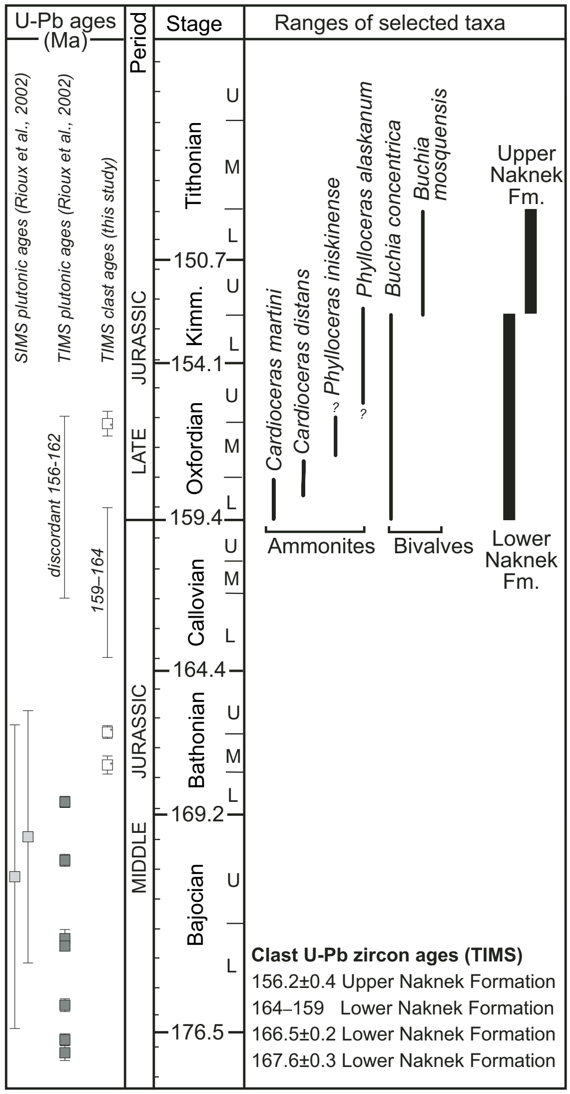

Figure 3. Stratigraphic chart showing age ranges of diagnostic megafossils recovered from the Naknek Formation, U-Pb ages of plutonic clasts from the Naknek Formation, and U-Pb ages of plutons in the Talkeetna Mountains. Megafossils are from this study (Tables DR1–DR2; Fig. DR-1) and from Imlay (1981). See Figure 5 for fossil locations within stratigraphic sections. *Buchia* age ranges after Miller and Detterman (1985). See Table 1 for U-Pb data for plutonic clasts. U-Pb ages of plutons from Rioux et al. (2002). All U-Pb zircon errors are 2σ. Geologic time scale after Gradstein et al. (1994).

Fan-Delta Lithofacies Association

Conglomeratic outcrops of the fan-delta lithofacies association are exposed exclusively along the northern margin of the outcrop belt (Jn1 in Figs. 2, 4, and 5). The fan-delta lithofacies association has a maximum preserved thickness of 400 m, contains southward-directed paleocurrent indicators (Fig. 1B), and consists of five dominant lithofacies: A1–A5.

Lithofacies A1 consists of poorly sorted, disorganized, matrix- to clast-supported pebble-cobble-boulder conglomerate (Figs. 7A and 7B). Subangular to subrounded clasts are encased by a poorly sorted matrix of sandstone and sparse mudstone. Boulders 1–2.5 m long are common. Individual beds are laterally persistent for several tens of meters. Most conglomerate beds have nonerosive bases and lack stratification but locally exhibit inverse grading. Lithofacies A1 is interpreted as being deposits of debris flows, hyperconcentrated flows, and fluidal sediment flows. Poor sorting, sand matrix, and limited clay content suggest deposition mainly by cohesionless debris flows in which clast support was maintained through frictional dispersion from high basal shear stresses and clast buoyancy related to high sediment concentrations (e.g., Nemec and Steel, 1984).

Lithofacies A2 is nongraded, clast-supported, pebble-cobble conglomerate. Clasts are subrounded to well rounded and moderately sorted. Most beds are structureless, but horizontal stratification and clast imbrication are present locally. Broadly lenticular over several tens of meters, individual beds are medium to thick bedded and contain belemnite fossils. Lithofacies A2 represents high-density, noncohesive debris flows transitional to hyperconcentrated flows (e.g., Lowe, 1982) that may have moved as pulsating surges (Nemec and Steel, 1984). The high clast concentration and lack of grading indicate that dispersive pressure played an important role in flow processes and that turbulence did not play a major role in supporting clasts.

Lithofacies A3 comprises inverse to normally graded, pebble-cobble conglomerate. Clasts are angular to rounded and poorly to moderately sorted. Matrix is dominated by medium- to coarse-grained sandstone. Beds are broadly lenticular and medium to thick bedded with sharp bed bases. Lithofacies A3 was deposited by currents transitional between grain flow and turbulent flow. Initially, inversely graded traction carpets formed due to high dis-

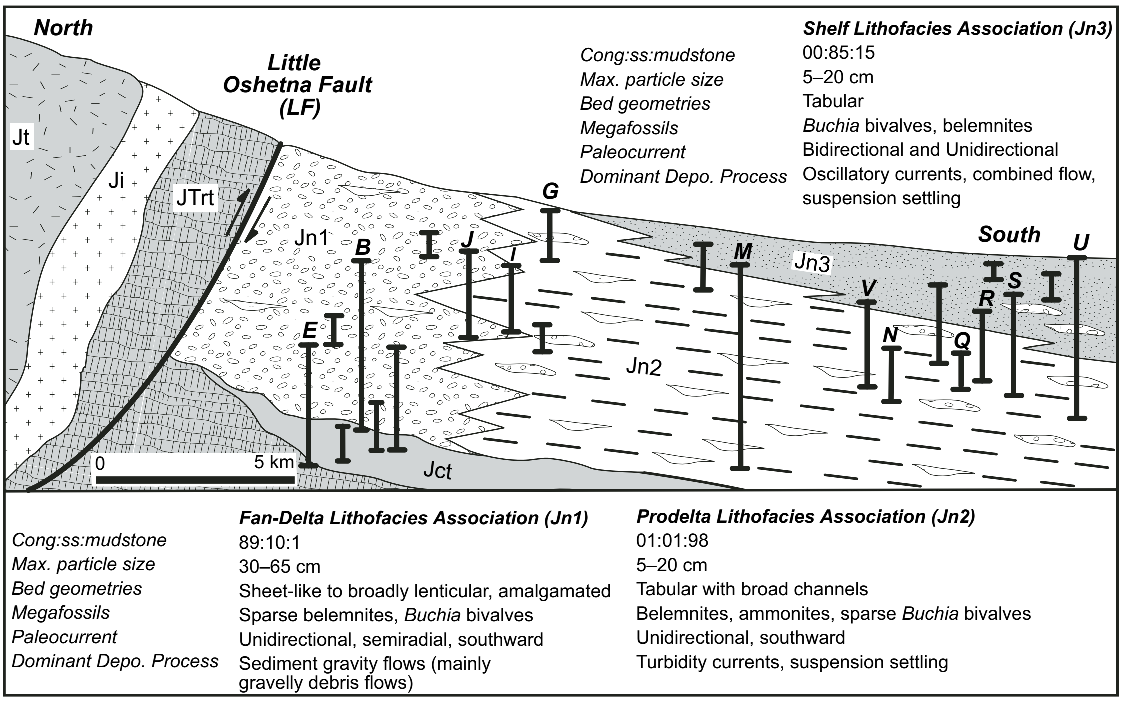

Figure 4. Schematic cross section showing generalized lateral and vertical relations between lithofacies associations. Vertical bold lines indicate position of measured stratigraphic sections. Representative sections (lettered) are shown in Figure 5. Maximum particle size (MPS) data were calculated from the average diameter of the ten largest clasts within individual conglomerate beds. Note distinct southward decrease in grain size from Jn1 to Jn2. See Figures 1B and 2 for explanation of abbreviations.

persive pressures. In later stages of flow, fluid turbulence became the major mechanism of sediment support with deposition occurring via suspension settling from high-density turbidity currents (e.g., Surlyk, 1984).

Lithofacies A4 consists of clast-supported, nongraded, granule-pebble conglomerate. Clasts are subrounded to rounded and moderately to well sorted. Beds are lenticular over 20–60 m, are medium bedded, have sharp bed bases, and contain belemnite fossils. Lithofacies A4 represents deposits of high-density debris flows and turbidity currents judging by the tight packing of conglomerate clasts and lack of sedimentary structures (e.g., Lowe, 1982; Nemec and Steel, 1984).

Lithofacies A5, a minor component of the fan-delta facies association, consists of massive, unstratified sandstone and mudstone. Sandstones are fine to coarse grained and moderately sorted. Beds are thin to thick and are broadly lenticular. Lithofacies A5 represents suspension settling from sediment gravity flows related to lithofacies A1–A4 and from buoyantly supported, midwater to surface plumes (e.g., Stow and Piper, 1984; Pickering et al., 1986).

In summary, lithofacies A1–A5 are dominated by conglomerate interpreted as the deposits of grain flows, debris flows, hyperconcentrated flows, and turbidity currents. The dominance of gravelly sediment-gravity-flow deposits, sparse marine megafossils, and southward-directed paleocurrent indicators suggests submarine deposition on an unstable, high-gradient, south-dipping basin floor. The limited proximal-distal extent (3–5 km) and broad lateral extent (40 km) of this facies association (Grantz, 1960a, 1960b) in combination with southward interfingering with finer-grained prodelta sediment gravity flow deposits (lithofacies B1–B4; Jn2 in Fig. 2) indicates deposition on coalesced gravelly fan deltas (e.g., Nemec and Steel, 1984; Postma, 1990).

Prodelta Lithofacies Association

Deposits of the prodelta lithofacies association (Jn2 in Figs. 2, 4, and 5) have a maximum preserved thickness of ~690 m, grade northward into the fan-delta lithofacies association (Jn1 in Figs. 2, 4, and 5), and are characterized by four dominant lithofacies: B1–B4. Submarine channels are common within the prodelta lithofacies association at sections L, M, and N (Fig. 2). Channels are 15–50 m wide and 5–20 m deep with northwest-southeast- to north-south–trending axes that widen southward over several hundred meters. Lithofacies B1–B4 are preserved within the channel complexes as well as interchannel regions.

Lithofacies B1 consists of nongraded, pebble-cobble conglomerate beds that are one to a few clasts thick (Fig. 5). A matrix of mudstone and fine-grained sandstone supports randomly oriented, subrounded clasts. Individual beds are laterally persistent and transform basinward (southward) into mudstone with isolated clasts. Lithofacies B1 is interpreted as gravitationally driven, near-bed movement of clasts, individually or as part of a group (debris fall, sensu Nemec, 1990). Downslope transitions from units a few clasts thick to isolated clasts in a mud matrix indicate flow transformations from grain-assemblage debris falls to single-grain debris falls (e.g., Sohn et al., 1997). Beds that are multiple clasts thick probably resulted from saltating gravel clasts, whereas beds only a single clast thick likely resulted from rolling or sliding of individual clasts with infrequent or no clast collisions.

Lithofacies B2 comprises of thin- to medium-bedded, very fine- to very coarse-grained sandstone (Figs. 7C–7F). Most thin-bedded sandstones are normally graded, whereas medium-bedded sandstones are nongraded to crudely normally graded. Internally, most beds are structureless, although parallel laminae, dish structures, and ripple-cross-laminated cappings are present locally. Sandstones have

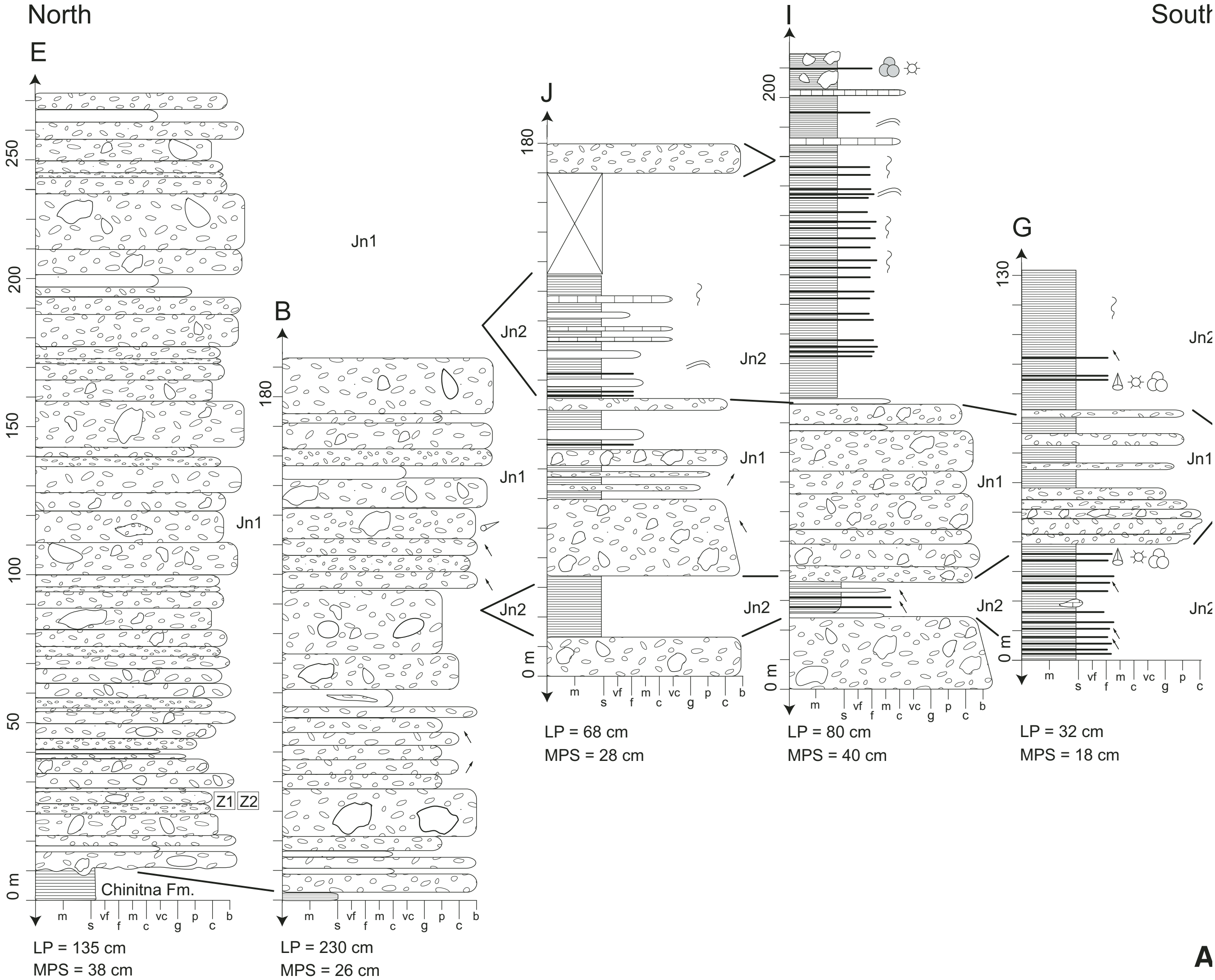

Figure 5. Logs of representative measured stratigraphic sections of the Naknek Formation. Sections were measured on a bed-by-bed basis using a Jacob staff. See Figures 2 and 4 for section locations and abbreviations. MPS—average diameter of the ten largest clasts within individual conglomerate beds; LP—largest single clast size from conglomerate within the measured section. Note lateral facies change in the lower Naknek Formation from northern conglomerate (Jn1) interpreted as fan-delta mass flows to southern sandstone and mudstone (Jn2) interpreted as prodelta turbidity current and suspension settling deposits. (*Continued on following page.*)

sharp, low-relief bases and are laterally persistent for several tens to hundreds of meters (Figs. 7C–7D). Fragments of belemnite and *Buchia* bivalve fossils are common. Lithofacies B2 represents the deposits of low- to high-density turbidity currents and minor debris flows produced partly by dilution and bypassing of gravelly mass flows that deposited their gravel fraction in more proximal (northern) environments (e.g., Nemec, 1990).

Lithofacies B3 consists of thin-bedded micritic limestone. Beds are sharp based, massive to laminar, tabular, and laterally persistent for tens to hundreds of meters. Limestone beds contain horizontal burrows as well as sparse bivalve, belemnite, and ammonite fossils that are typically whole and articulated. Lithofacies B3 records suspension settling of calcareous marine clay and silt.

Lithofacies B4 is of gray to black, amalgamated mudstone sequences that are laterally persistent for hundreds of meters (Figs. 7C–7E). Sedimentary structures are generally lacking due to bioturbation and weathering, although faint parallel laminae are preserved locally. Radiolaria and thick-walled, agglutinated foraminifera are prevalent (Fig. 5). Calcareous concretions contained in the mudstones are aligned parallel to bedding and contain whole ammonite fossils. Lithofacies B4 represents suspension settling of fine-grained sediment from the tails of turbidity currents and buoyantly supported, midwater to surface plumes (e.g., Stow and Piper, 1984; Pickering et al., 1986).

In summary, lithofacies B1–B4 are dominated by interbedded mudstone and sandstone interpreted as slow suspension settling of mud during fair-weather conditions (B3, B4) and rapid deposition by turbidity currents (B2) and debris falls (B1). The prevalence of mudstone and sandy turbidity current deposits, marine fossils, and minor channels indicate submarine deposition on a relatively steep, channelized basin floor. The north-south trend of submarine channels, southward fining of lithofacies A1,

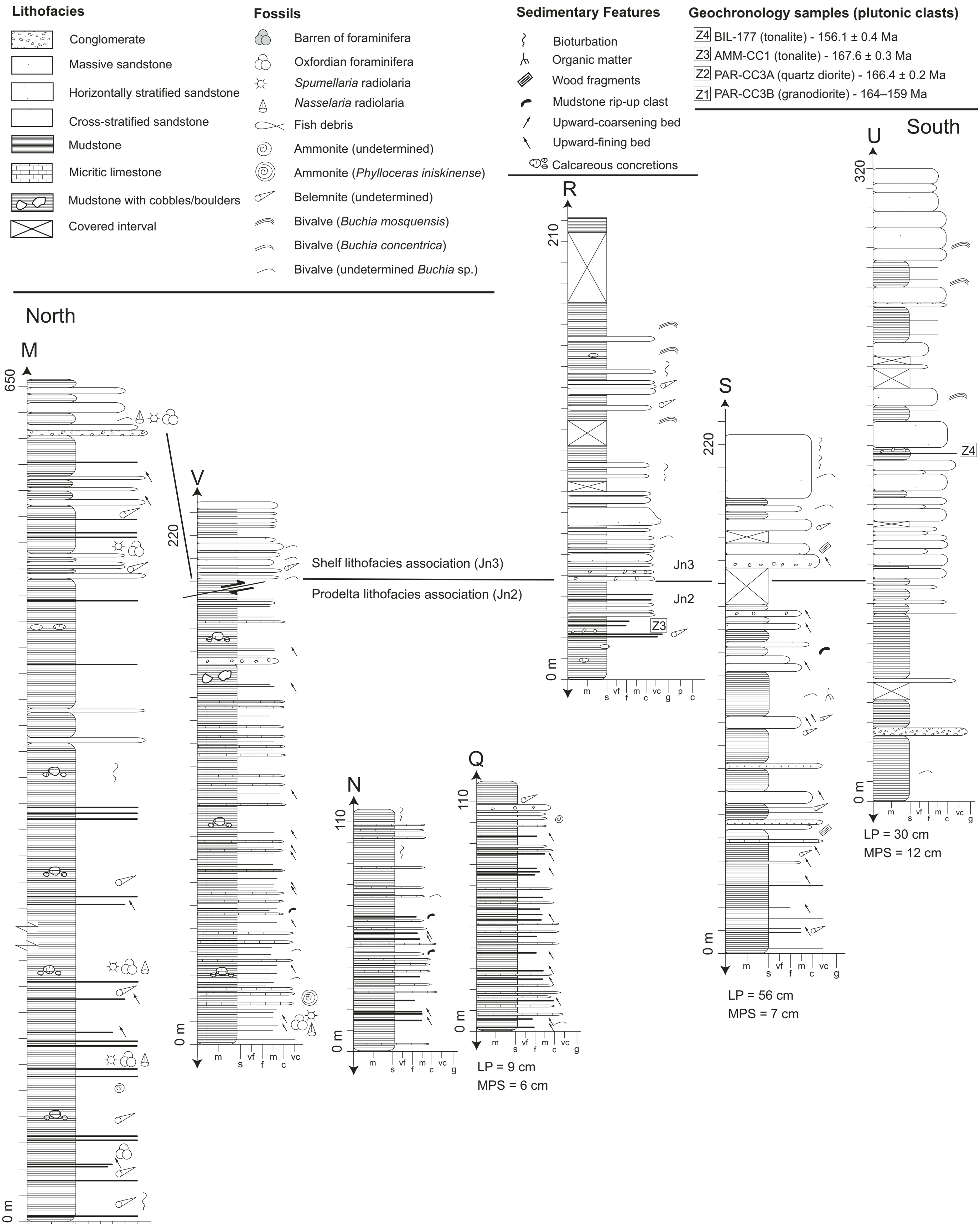

Figure 5 (*continued*).

TABLE 1. U-PB ZIRCON AGE DATA FOR PLUTONIC CLASTS FROM NAKNEK FORMATION CONGLOMERATE, TALKEETNA MOUNTAINS, ALASKA

Step	Step T†	wt.‡	U§	% tot. U#	Isotopic ratios						Ages (Ma)					
					^{208}Pb/^{206}Pb††	^{204}Pb/^{206}Pb††	^{207}Pb*/^{206}Pb*‡‡		^{206}Pb*/^{238}U6		^{206}Pb/^{238}U§§	2σ	^{207}Pb/^{235}U§§	2σ	^{207}Pb/^{206}Pb§§	2σ
Bil 1–177 (6.75 mg, 144 ppm U)##																
a	160	0.30	1007	31.7	0.1347	0.00221	0.05017	(1.7)	0.023452	(0.3)	149.4	0.3	152.6	2.6	202.8	39.7
b	170	0.31	302	9.6	0.06824	0.0000606	0.04945	(0.11)	0.024412	(0.3)	155.5	0.3	156.3	0.5	169.1	2.5
c	180	0.73	184	14.0	0.07723	0.0000595	0.04934	(0.11)	0.024479	(0.3)	155.9	0.3	156.4	0.5	163.9	2.5
d	180	1.23	113	14.3	0.08838	0.0000530	0.049337	(0.07)	0.024543	(0.3)	156.3	0.3	156.8	0.5	163.9	1.6
e	190	1.28	84	11.1	0.09801	0.0000354	0.049230	(0.10)	0.024577	(0.3)	156.5	0.3	156.7	0.5	158.8	2.3
f	190	1.32	70	9.5	0.1074	0.0000653	0.049271	(0.11)	0.024463	(0.3)	155.8	0.3	156.1	0.5	160.7	2.7
g	RES	1.58	61	9.9	0.1143	0.0000355	0.049319	(0.08)	0.024553	(0.3)	156.4	0.3	156.8	0.5	163.0	2.0
Sample age†††											156.2	0.4	(weighted mean of steps c–g)			
AMM CC-1 (1.65 mg, 217 ppm U)##																
a	160	0.04	460	5.5	0.4364	0.00899	0.0479	(8.6)	0.024061	(1.2)	153.3	0.3	149.7	13.0	93.4	205.7
b	170	0.11	319	9.8	0.1025	0.000113	0.04970	(0.25)	0.026101	(0.3)	166.1	0.3	167.1	0.6	181.1	5.9
c	180	0.35	210	20.7	0.1189	0.0000391	0.049611	(0.10)	0.026305	(0.3)	167.4	0.3	168.0	0.5	176.8	2.5
d	180	0.35	199	19.3	0.1332	0.0000427	0.049515	(0.11)	0.026345	(0.3)	167.6	0.3	167.9	0.5	172.3	2.7
e	190	0.50	203	28.1	0.1412	0.0000389	0.049495	(0.07)	0.026379	(0.3)	167.8	0.3	168.1	0.5	171.3	1.7
f	RES	0.30	197	16.6	0.1487	0.0000497	0.049487	(0.15)	0.026347	(0.3)	167.6	0.3	167.9	0.6	171.0	3.5
Sample age†††											167.6	0.3	(weighted mean of steps c–f)			
Par CC3-a (1.84 mg, 411 ppm U)##																
a	160	0.11	2668	38.4	0.1162	0.000701	0.04955	(0.52)	0.024290	(0.3)	154.7	0.3	155.9	0.9	173.7	12.4
b	170	0.18	607	14.0	0.1088	0.0000242	0.049578	(0.07)	0.026193	(0.3)	166.7	0.3	167.2	0.5	175.3	1.7
c	180	0.50	320	21.0	0.1212	0.0000197	0.049408	(0.08)	0.026179	(0.3)	166.6	0.3	166.6	0.5	167.3	2.0
d	180	0.54	186	13.2	0.1276	0.0000306	0.049515	(0.10)	0.026102	(0.3)	166.1	0.3	166.5	0.5	172.3	2.3
e	190	0.36	189	8.9	0.1337	0.0000385	0.049503	(0.09)	0.026158	(0.3)	166.5	0.3	166.8	0.5	171.7	2.3
f	RES	0.16	203	4.4	0.1425	0.000117	0.04940	(0.28)	0.026169	(0.5)	166.5	0.3	166.6	1.1	167.1	6.6
Sample age†††											166.5	0.2	(weighted mean of steps b–f)			
Par CC3-b (0.14 mg, 239 ppm U)##																
a	160	0.01	1432	24.5	0.5374	0.0126	0.0495	(13)	0.02285	(1.8)	145.6	0.5	147.2	19.6	173.3	314.4
b	170	0.01	433	17.8	0.1294	0.000379	0.04832	(1.2)	0.02574	(0.5)	163.8	0.5	160.7	2.1	115.0	28.9
c	180	0.04	213	26.8	0.2343	0.00302	0.0500	(2.5)	0.02575	(0.5)	163.9	0.5	166.0	4.2	197.0	59.0
d	180	0.04	134	14.9	0.1451	0.000598	0.05056	(1.3)	0.02555	(0.5)	162.6	0.5	166.4	2.4	220.6	32.2
e	RES	0.04	132	16.0	0.1543	0.000571	0.04831	(2.0)	0.02505	(0.5)	159.5	0.5	156.7	3.2	114.7	46.8
Sample age†††											164–159					

†Samples were analyzed using the chemical abrasion technique developed by Mattinson (2001a, 2001b, 2003). For each sample, one zircon fraction was annealed at 900ºC for 48 h and then dissolved in 5–7 discrete steps. Digestion temperatures are listed in column 1. Low temperature clean-up steps (steps a and b) are intended to preferentially remove high U layers in the zircon population that are effected by extensive radiation damage and secondary Pb loss. All digestions were done in a ~10: 1 HF-HNO_3 solution. RES indicates total digestion of the final zircon residue. Uranium and Pb were separated using standard ion exchange columns miniaturized after Krogh (1973) and analyzed on the Finnigan MAT-261 at the University of California, Santa Barbara.

‡Weight (mg) of zircon dissolved in each digestion step. Weights were determined by ICP-ES analysis of sample solutions and are accurate to ~10%.

§Uranium concentrations (ppm) of dissolved zircon.

#Percentage of the total U released by each step.

††Observed isotopic ratios corrected for fractionation based on replicate analyses of NBS Pb standard 983, and corrected for ^{208}Pb, ^{207}Pb, ^{206}Pb, ^{204}Pb, ^{238}U, and ^{235}U in the ^{205}Pb/^{235}U spike.

‡‡Radiogenic ^{207}Pb/^{206}Pb and ^{206}Pb/^{238}U ratios corrected for fractionation (see above), spike composition, and common Pb isotopic values of ^{207}Pb/^{204}Pb = 15.6 and ^{206}Pb/^{204}Pb = 18.7. The reported ^{207}Pb/^{206}Pb and ^{206}Pb/^{238}U ratios are additionally corrected for initial exclusion of 80% of the ^{230}Th from the ^{238}U decay chain. Two sigma errors, shown in parentheses, follow Mattinson (1987).

§§Ages (Ma) calculated using ^{238}U/^{235}U = 137.88 and decay constants of ^{238}U = 1.5513×10^{-10} yr^{-1} and ^{235}U = 9.8485×10^{-10} yr^{-1}. All ^{207}Pb/^{206}Pb ages were calculated with the Isoplot/Ex program developed by Ludwig (1999). Age uncertainties are 2σ absolute errors.

##Weight and U content of the total zircon fraction used in the chemical abrasion analysis.

†††Weighted mean of the ^{238}U/^{206}Pb ages excluding low temperature clean-up steps. For Par CC-3b the high temperature steps do not define a single age but suggest a crystallization age between 164 and 159 Ma.

and northward interfingering of lithofacies B1–B5 with conglomeratic mass flows of lithofacies A1–A5 suggest deposition on a southward-dipping prodelta slope characterized by episodic sediment gravity flows.

Siliciclastic Shelf Lithofacies Association

The shelf lithofacies association has a maximum preserved thickness of ~255 m, depositionally overlies the prodelta lithofacies association (Fig. 7G), and includes three main lithofacies: C1–C3 (Jn3 in Figs. 2, 4, and 5).

Lithofacies C1 consists of medium- to coarse-grained, nongraded to stratified sandstone. Grains are subrounded to rounded and moderately sorted. Sedimentary structures include horizontal stratification, planar and trough cross-stratification, and symmetrical ripple stratification. Sandstones are medium to thick bedded, tabular, and amalgamated (Fig. 7G); bioturbated mudstones locally separate sandstone beds (Fig. 7H). Disarticulated *Buchia* bivalve megafossils and subvertical biogenic structures are common. Lithofacies C1 represents shallow marine sandstone deposited as bedload traction currents in shoreface to inner siliciclastic shelf environments. The prevalence of horizontal stratification and *Buchia* fossils indicates deposition under high-energy conditions above normal wave base.

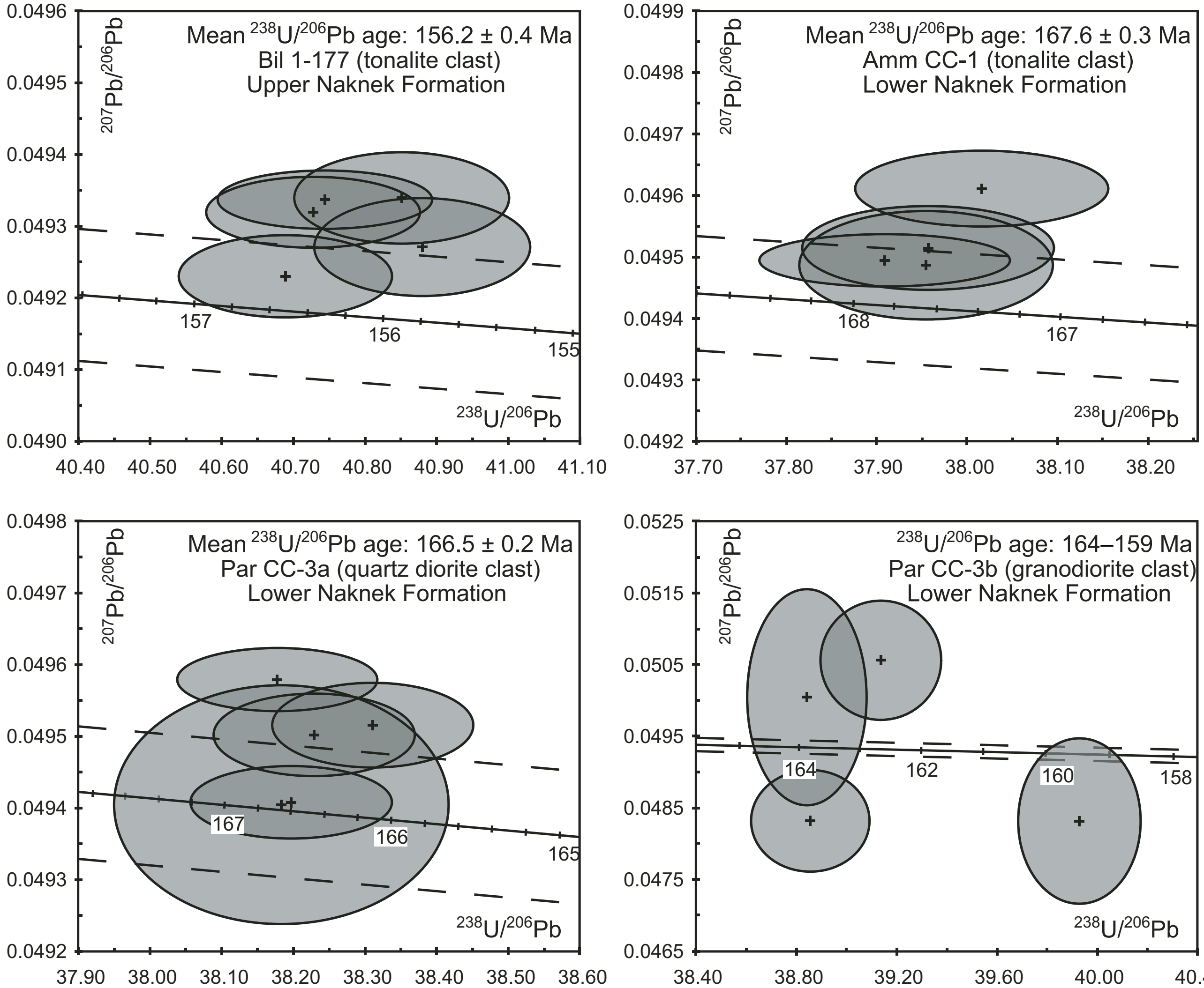

Figure 6. Tera-Wasserburg concordia diagrams for zircon separates from individual plutonic clasts in the Naknek Formation. See Table 1 for analytical details and raw data. Clast ages are similar to U-Pb zircon ages from Jurassic plutons in the Talkeetna Mountains (177–156 Ma; Rioux et al., 2002). Concordia plots show the high temperature digestion steps from the four chemical abrasion analyses. The weighted mean of the high temperature steps from Bil 1–177, AMM CC-1, and Par CC-3a are interpreted as concordant crystallization ages. The data from sample Par CC-3b are consistent with a crystallization age between 164 and 159 Ma, but the spread in the data and the slight discordance may result from a minor component of inherited zircon. All error ellipses are 2σ. Dashed lines show 2σ uncertainties in concordia based on decay constant uncertainties of ^{238}U = 0.107 and ^{235}U = 0.136 (Jaffey et al., 1971). Concordia diagrams were produced using the Isoplot/Ex program developed by Ludwig (1999).

Lithofacies C2 consists of highly variable beds that contain massive concentrations of calcareous fossil shell material with a range of preservation and taphonomic features. Most shell beds are 5–25 cm thick and broadly lenticular with nonerosive bases. Shells of *Buchia* bivalves are dominant and range from whole articulated valves indicative of life position to broken and abraded fragments suggestive of relatively high energy concomitant with transport. Some units include coquinoid *Buchia* bivalve accumulations with large numbers of disarticulated valves and a proportion of articulated specimens densely packed within a matrix of sandstone and shell hash (Fig. 7J). Articulated, life-position bivalves commonly occupy the upper part of individual shell beds. The preserved bivalve fauna is typical of shallow, high-energy marine environments (e.g., Miller and Detterman, 1985). Taphonomic features indicate alternating conditions between episodes of reduced sediment influx and storm sedimentation (e.g., Kidwell, 1991).

Lithofacies C3 comprises massive siltstone. Siltstones are gray, black, or tan, and range from noncalcareous to calcareous. Bedding and stratification are rarely preserved as a result of bioturbation and weathering. Individual beds are amalgamated into monotonous sequences up to 20 m thick (Fig. 7I). Abundant bivalve, belemnite, and ammonite fossils are dominantly whole and articulated. Lithofacies C3 records suspension settling of clay and silt from buoyantly supported midwater- and/or surface-plumes in open-marine environments (e.g., Stow and Piper, 1984; Pickering et al., 1986).

In summary, lithofacies C1–C3 is dominated by cross-stratified sandstone, coquina, and mudstone deposited by oscillatory currents and

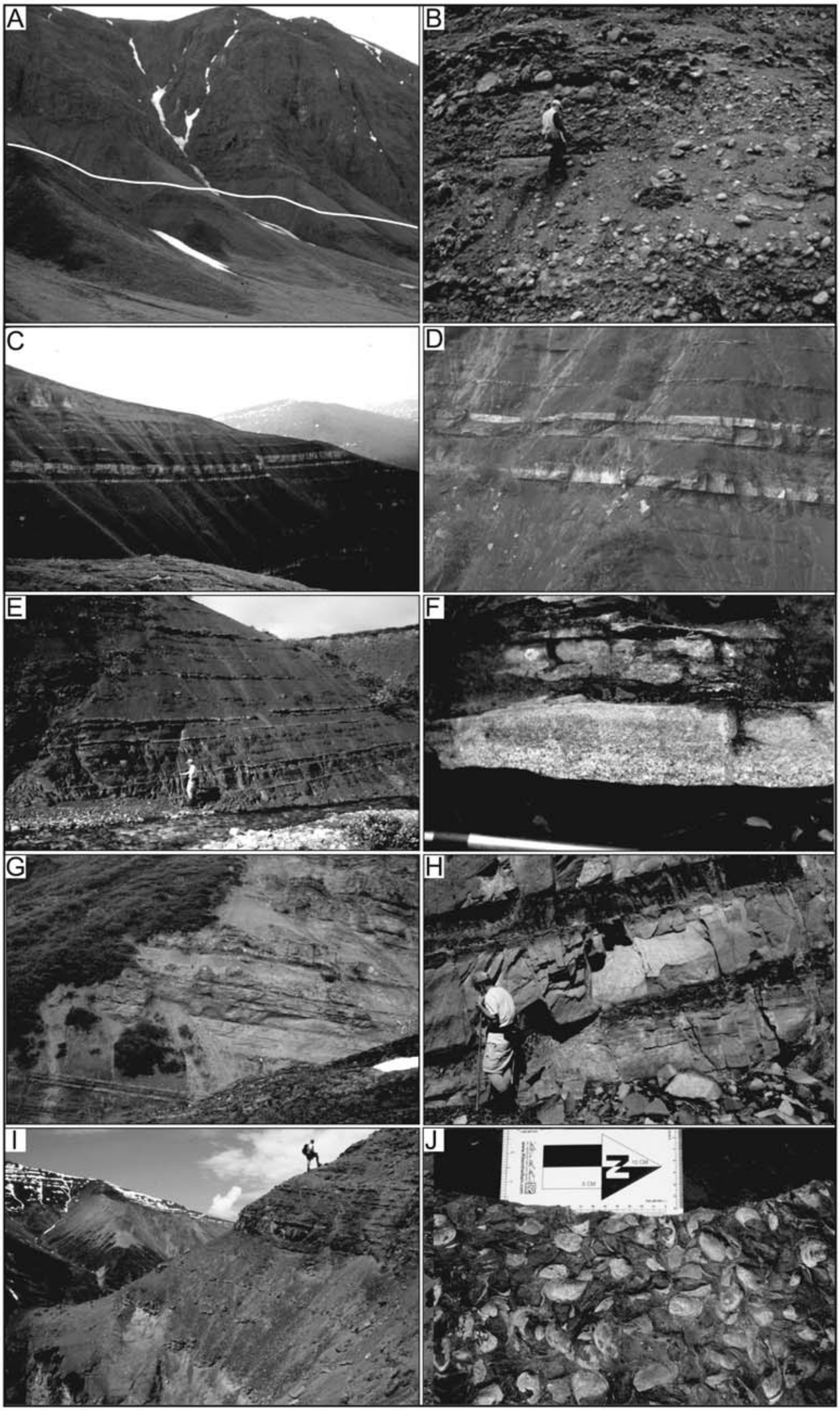

Figure 7. Photographs of fan-delta (A–B), prodelta (C–F), and shelf (G–J) lithofacies associations of the Naknek Formation. See Figures 2 and 5 for section locations. (A) Disconformity (white line) separating uppermost Chinitna Formation and lowermost Naknek Formation at section B. Naknek Formation outcrop is ~400 m thick and consists of boulder-cobble conglomerate. (B) Poorly to moderately sorted conglomerate at section H. Individual conglomerate beds are inversely graded locally (e.g., knee to head of person). (C) Mudstone (dark units) and laterally persistent massive sandstone (light units) in middle of section S. Outcrop is 200 m thick. (D) Mudstone (dark recessive units) and laterally persistent massive sandstone beds (light units) near base of section R. Person (center) is standing next to 80-cm-thick, sharp-based, normally graded sandstone bed. (E) Thin-bedded, sharp-based sandstones (light units) and massive black mudstone at section V. Person (left center) for scale. (F) Close-up of sharp-based, normally graded sandstone shown in (E). Pencil for scale. (G) Transition from prodelta (Jn2) to siliciclastic shelf (Jn3) lithofacies association at section U. Note black mudstone and thin-bedded, laterally persistent sandstone in upper part of prodelta lithofacies (lower left) and amalgamated massive sandstone beds in shelf lithofacies (upper right). Person (lower right) for scale. (H) Close-up of massive sandstone (light units) and thin, interbedded mudstone (dark units) of shelf lithofacies association at section V. (I) Mudstone with calcareous concretions and thin-bedded massive sandstone of the uppermost Naknek Formation (lithofacies association F4 at section U). Person (upper right) for scale. (J) Shell bed containing dense accumulation of *Buchia mosquensis* bivalve fossils from section T. Length of scale is 10 cm.

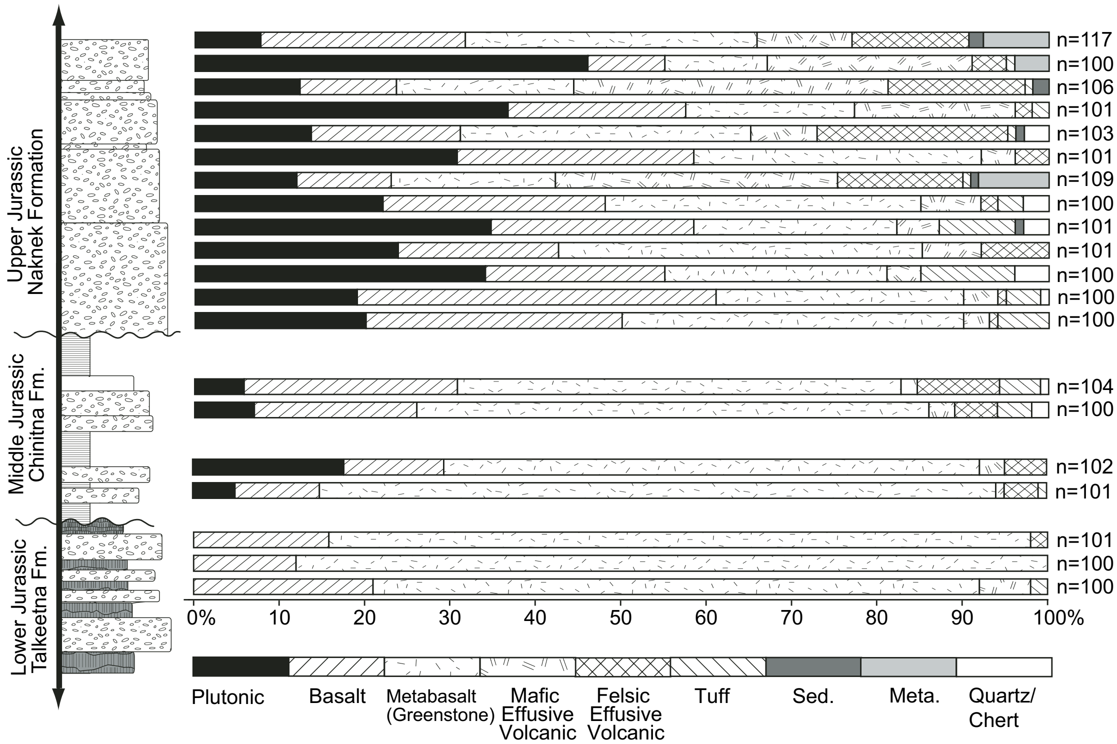

Figure 8. Histograms showing stratigraphic variation in composition of Lower to Upper Jurassic conglomerates in the southeastern Talkeetna Mountains. n—number of clasts counted. Clast counts from the Naknek Formation are exclusively from proximal (northern) sections (B through I in Fig. 2). Clast counts from the Talkeetna and Chinitna Formations are from sections A and E in Figure 2. Note dominance of igneous clast types and upsection increase in plutonic detritus from Lower Jurassic to Upper Jurassic conglomerates. Lower Jurassic conglomerates are completely devoid of plutonic clasts. Middle Jurassic conglomerates contain sparse plutonic clasts (5%–18%; mean = 8%). Late Jurassic conglomerates contain more abundant plutonic clasts (9%–42%; mean = 24%). See text for description of clast types.

combined flow (A1 and A2) as well as suspension settling (A3). The prevalence of open-marine megafossils, coquina, and wave-formed sedimentary structures in combination with the absence of sediment gravity flow deposits indicates deposition on a marine shelf above storm-wave base.

Compositional and Provenance Data

Quantitative provenance data have not been reported previously from the Naknek Formation in the Talkeetna Mountains. New clast counts from conglomerate (n = 1,339), modal analysis of sandstone thin sections (n = 7), and U-Pb zircon geochronology of plutonic clasts (n = 4) document source terranes that contributed detritus during Late Jurassic sedimentation. Compositional data were obtained from conglomerate beds in the field by tabulating the lithology of all pebble-, cobble-, and boulder-sized clasts within a 1–5 m^2 outcrop face, yielding a minimum population of 100 clasts per bed. Samples were also collected from potential source terranes and thin sections were prepared to compare clast types with inferred source rocks. Megascopic field identifications were checked through thin-section analysis of representative samples of each clast type. Conglomerate compositional data are presented in Figure 8 according to relative stratigraphic position. See Szuch (2002) for raw clast count data and detailed petrographic descriptions of clasts and source terranes. Thin sections of medium-grained sandstones from a continuous measured section (M in Fig. 5) were point counted. See Table 2 for point-counting parameters and recalculated point-count data. Point-count methods and data are presented in Table DR3.

Conglomerate Data

Conglomerates of the Naknek Formation are polymictic and moderately to poorly sorted with subangular to rounded clasts. Conglomerates consist almost exclusively of igneous clast types (96% of total population), including volcanic (72%) and plutonic (24%) varieties. Plutonic clast types are dominated by felsic varieties, including hornblende-biotite granite, hornblende-biotite quartz diorite, granodiorite, tonalite, quartz diorite, granite, and quartz monzonite. Effusive volcanic clast types are dominated by mafic varieties that comprise three groups: basalt, greenstone, and mafic volcanic (Fig. 8; Fig. DR2). Basalt clasts include gray, black, and gray-green varieties with aphanitic to aphanitic-porphyritic textures. Weakly foliated to nonfoliated greenstones are aphanitic to porphyritic and contain plagioclase phenocrysts that are altered to epidote and chlorite. Mafic nonbasalt clasts include porphyritic andesite, aphanitic andesite, and porphyritic basaltic andesite. Minor felsic effusive clasts include gray to brown rhyolite and gray dacite. Rare noneffusive volcanic clasts include gray-green siliceous tuff and gray crystal-vitric tuff. Minor sedimentary and metamorphic clasts are polymictic pebble conglomerate, feldspathic sandstone with *Buchia* bivalve fragments, black siltstone, gneiss, amphibolite, and phyllite. Sparse siliceous clasts consist of white, massive quartz and black, gray, and green chert.

TABLE 2. RECALCULATED MODAL POINT-COUNT DATA FROM THE NAKNEK FORMATION

Sample	Q	F	L	Lv	Ls	Lm	Qm	P	K	Lv	F	DO
M-632	0.01	0.94	0.05	0.94	0.00	0.06	0.01	0.99	0.00	0.04	0.83	0.13
M-517	0.03	0.93	0.04	1.00	0.00	0.00	0.03	0.97	0.00	0.03	0.81	0.16
M-282.75	0.00	0.93	0.07	1.00	0.00	0.00	0.00	0.99	0.01	0.06	0.79	0.15
M-119.5	0.02	0.97	0.01	1.00	0.00	0.00	0.02	0.98	0.00	0.01	0.86	0.13
M-53.0	0.02	0.90	0.08	1.00	0.00	0.00	0.02	0.94	0.04	0.07	0.83	0.10
M-44.6	0.01	0.99	0.00	1.00	0.00	0.00	0.01	0.99	0.00	0.00	0.95	0.05
M-20.25	0.01	0.99	0.00	1.00	0.00	0.00	0.01	0.99	0.00	0.00	0.94	0.06
Average	*0.01*	*0.95*	*0.04*	*0.99*	*0.00*	*0.01*	*0.01*	*0.98*	*0.01*	*0.03*	*0.86*	*0.11*
std	*0.01*	*0.03*	*0.03*	*0.02*	*0.00*	*0.02*	*0.01*	*0.02*	*0.01*	*0.03*	*0.06*	*0.04*

Notes: Sample numbers represent meters above base of Naknek Formation at measured section M in Figs. 2 and 5. Raw parameters: Qm—monocrystalline quartz; P—plagioclase feldspar; K—potassium feldspar; Lvl—lathwork volcanic lithic fragment; Lvf—felsic volcanic lithic fragment; Lvh—highly altered volcanic lithic fragment; Lmm—mica schist lithic fragment; Cp—clinopyroxene; Op—opaque minerals; Ol—olivine; Hn—hornblende; Sp—sphene. See Table DR3 for raw data. Recalculated parameters: Q—total quartzose grains (= Qm); F—total feldspar grains (= P + K); L—total unstable lithic grains (= Lvl + Lvf + Lvh + Lmm); Ls—total sedimentary lithic grains (none); Lm—total metamorphic lithic grains (= Lmm) Lv = total volcanic lithic grains (= Lvl + Lvf + Lvh); DO—total dense and opaque minerals grains (= Cp + Op + Ol + Hn + Sp).

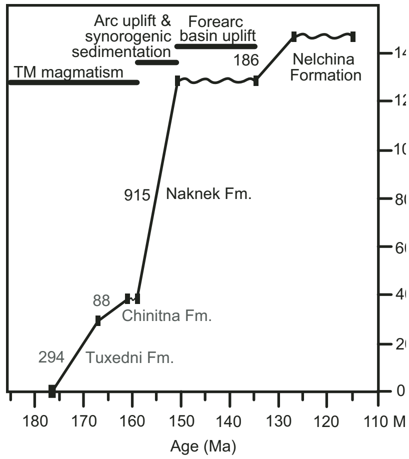

Figure 9. Stratigraphic thickness versus time plot for Middle Jurassic to Lower Cretaceous strata, southern Talkeetna Mountains. Wavy lines represent disconformities separating marine strata. TM magmatism represents emplacement of plutons in the southern Talkeetna Mountains; small open circles represent U-Pb zircon crystallization ages (n = 11; Rioux et al., 2002). Note rapid accumulation of conglomeratic Upper Jurassic Naknek Formation shortly following pluton emplacement.

Sandstone Data

Naknek Formation sandstones point counted for this study are medium grained and moderately sorted with subangular to subrounded framework grains. Sandstones are enriched in feldspar and have minor proportions of quartzose and lithic grains. Modal percentages are dominated by plagioclase feldspar, volcanic lithic grains, pyroxene, hornblende, and monocrystalline quartz. Mean modal compositions are $Q_1F_{95}L_4$, $Lv_{99}Ls_0Lm_1$, and $Qm_1P_{98}K_1$ (Table 2). Common framework grains are described below in order of decreasing abundance. Plagioclase feldspars are subangular with variable alteration; sericite and authigenic albite are common. Plagioclase feldspars are observed as individual grains or laths in volcanic lithic grains. Volcanic lithic grains are unaltered to highly altered and include three common varieties: (i) felsitic texture with subhedral to euhedral plagioclase and hornblende phenocrysts in a seriate groundmass; (ii) porphyritic lathwork texture with subhedral to euhedral plagioclase phenocrysts in an aphanitic felsic matrix; and (iii) felsitic texture with aphanitic plagioclase and chert. Unstable accessory minerals make up 11% of the modal composition and include euhedral to subhedral clinopyroxene, orthopyroxene, hornblende, olivine, magnetite, sphene, and zircon. Minor low-grade, phyllosilicate-rich metamorphic grains are biotite schist and phyllite. Sparse clastic sedimentary lithic grains are dominated by shale and coarse siltstone.

U-Pb Clast Geochronology

Four felsic plutonic clasts were selected from the lower and upper Naknek Formation for U-Pb geochronologic analyses. The stratigraphic positions of the geochronology samples are shown in Figure 5. One fraction from each clast was annealed and then digested in multiple stages, following the chemical abrasion technique developed by Mattinson (2001a, 2001b, 2003). Table 1 and Figure 6 show the geochronologic data and analytical details. Felsic plutonic clasts from the lower Naknek Formation yield concordant Middle Jurassic U-Pb zircon ages (167.6 ± 0.3 Ma; 166.5 ± 0.2 Ma, ca. 164–159 Ma). A felsic plutonic clast from the upper Naknek Formation yields an Upper Jurassic U-Pb zircon age (156.2 ± 0.4 Ma).

Provenance Summary

Compositional, geochronologic, and sedimentologic data from the Naknek Formation indicate derivation mainly from igneous source terranes that are presently exposed along the arcward (northern) margin of the forearc basin deposits. Paleocurrent indicators demonstrate consistent southward-directed sediment transport (Fig. 1B). Textural data show a progressive southward decrease in grain size from boulder- and cobble-sized clasts along the Little Oshetna fault to pebble-sized clasts in southern outcrops (Figs. 4 and 5). Lithofacies associations document southward transitions from proximal gravelly mass-flow deposits to distal turbidity-current deposits (Fig. 4). Igneous sources are indicated by the dominance of volcanic and plutonic clasts in the gravel fraction and the prevalence of feldspar, volcanic-lithic fragments, and unstable accessory minerals in the sand fraction. Detritus was most likely derived from plutonic and volcanic rocks presently exposed in the hanging wall of the Little Oshetna fault (LF in Fig. 1B), where Middle to Upper Jurassic felsic plutons (Ji and Jt in Fig. 1B) intrude the Talkeetna Formation, a 3,000-m-thick sequence of Lower Jurassic volcanic strata (JTrt in Figs. 1B and 2). Talkeetna Formation volcanic rocks exposed along the northern basin margin are dominated by mafic lava flows that are petrographically similar to basalt, andesite, and greenstone clasts contained in Naknek Formation conglomerate (Fig. DR2; Szuch, 2002). Felsic plutonic clasts yield concordant U-Pb zircon ages (Table 1; Figs. 5 and 6) that overlap U-Pb zircon ages from petrographically comparable plutonic source terranes (Figs. 3 and 9; Szuch, 2002; Rioux et al., 2002, 2003). Late Jurassic exhumation of the felsic plutons is supported by K-Ar and Ar-Ar ages (174–143 Ma; Csejtey et al., 1978; P.W. Layer, 2003, personal commun.) that record cooling of the plutons through the biotite closure temperature contemporaneous with conglomerate deposition. The outsized nature of plutonic clasts in the conglomerates in combination with the paucity of quartzose framework grains in sandstone suggest relatively minor reworking of plutonic debris prior to deposition. Exhumation of the felsic plutons is also indicated by progressive upsection increases in the proportion of plutonic clasts in Lower Jurassic (0%), Middle Jurassic (8%), and Upper Jurassic (24%) conglomerate. These data support previous mapping studies that reported upsection increases in plutonic detritus in Middle to Upper Jurassic sedimentary strata and inferred derivation from northern igneous sources (e.g., Grantz et al., 1963; Winkler, 1992; Detterman et al., 1996). Minor sedimentary and metamorphic clasts contained

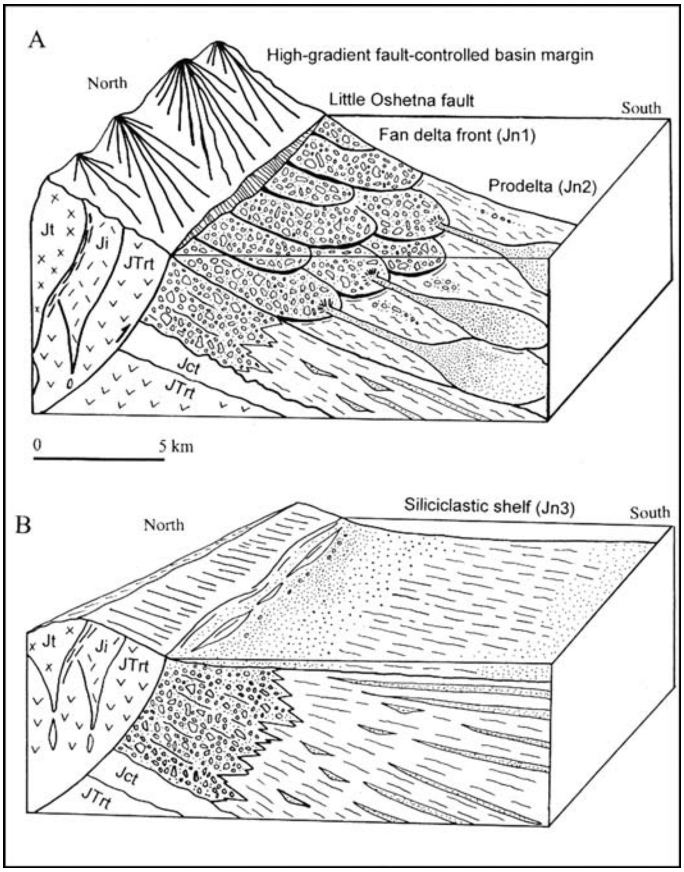

Figure 10. Schematic block diagrams showing preferred depositional model of the Naknek Formation during early to late Oxfordian (A) and early Kimmeridgian–early Tithonian (B) time. Nonmarine depositional environments are not illustrated because facies from those environments are not preserved or exposed. The position of the Little Oshetna fault is tentatively inferred to be near the shoreline based on the steep marine depositional gradients, lack of preserved nonmarine strata, and Late Jurassic sea level highstand, which was up to 100 m higher than present (Haq et al., 1988). Stratigraphic data do not preclude a nonmarine position for the fault. See text for discussion. See Figures 1B and 2 for explanation of abbreviations.

in the Naknek Formation are not source diagnostic but are consistent with derivation from local northern source terranes. Metamorphic clasts are petrographically similar to pendants exposed on the margins of the felsic plutons (Jm in Fig. 1B). Sedimentary clasts represent reworked deposits of the Chinitna and Naknek Formation based on the similarities in texture, framework grains, and *Buchia* bivalve fossil fragments.

DISCUSSION

Late Jurassic Forearc Basin Development

Figures 10–11 show our preferred model of Late Jurassic–Early Cretaceous forearc basin development in the Talkeetna Mountains based on our new data from the Naknek Formation. This model includes the following three phases: (1) initial rapid sedimentation on a high-gradient depositional slope characterized by coarse-grained marine sediment gravity flows; (2) relative sea-level decrease and siliciclastic shelf deposition; and (3) postdepositional basin floor uplift, unconformity development, and dextral strike-slip deformation.

Phase 1—Deep-Water Fan-Delta Sedimentation (Lower Naknek Formation)

During early Oxfordian to early Kimmeridgian time (ca. 159–153 Ma), the lower Naknek Formation was deposited disconformably above Middle Jurassic (Callovian) fine-grained marine strata. Deposition of the Naknek Formation marked a pronounced increase in grain size and sedimentation rates relative to Middle Jurassic deposition (Fig. 9). Coarse-grained sediment was transported southward along a high-gradient northern basin margin characterized by deep-water fan deltas (Fig. 10A). Proximal, gravelly debris flows and grain flows transformed downslope into sandy turbidity currents on a channelized prodelta slope. A dominantly submarine origin is indicated by the encasement of mass-flow deposits within marine fossil-bearing lithofacies and the lack of features indicating subaerial deposition (i.e., paleosols, desiccation features). Southward-directed paleocurrent indicators, southward decreases in grain size, detrital zircon ages, and compositional data indicate that detritus was derived mainly from Jurassic volcanic and plutonic source terranes exposed along the northern basin margin. Relatively high denudation rates in combination with steep depositional gradients prompted deposition of poorly sorted gravels with abundant meter-size plutonic clasts and sand enriched in feldspar, hornblende, and pyroxene. Accumulation of several hundred meters of boulder-rich mass-flow conglomerate in the footwall of the Little Oshetna fault contemporaneous with exhumation in the hanging wall suggests syndepositional displacement. Diagnostic evidence for syndepositional footwall rotation (e.g., growth strata) has not been recognized. Ancient deep-water fan deltas comparable to the lower Naknek Formation are reported from eustatic highstands (see Higgs, 1990, for review), including Late Jurassic highstands (e.g., Stow et al., 1982; Surlyk, 1984).

Phase 2—Shelf Sedimentation (Upper Naknek Formation)

Sediment gravity flow deposits of the lower Naknek Formation were onlapped by shallow-marine shelf strata of the upper Naknek Formation indicating a decrease in depositional gradients during Kimmeridgian time. Sedimentation was characterized by a combination of tractive transport and suspension settling processes, typically above storm-wave base (Fig. 10B). Continued exhumation of felsic plutons in the Talkeetna Mountains is indicated by a U-Pb zircon age (156.2 ± 0.4 Ma) of a plutonic clast from the upper Naknek Formation, which contains early Kimmeridgian to early Tithonian megafossils (ca. 153–149 Ma).

Phase 3—Postdepositional Uplift And Strike-Slip Displacement

The upper Naknek Formation was onlapped by Lower Cretaceous shallow marine sedimentary strata across a disconformity that records a 10–15 m.y. hiatus (Fig. 9). The lack of significant angular discordance across the unconformity indicates that the forearc basin was subaerially uplifted and exposed but not

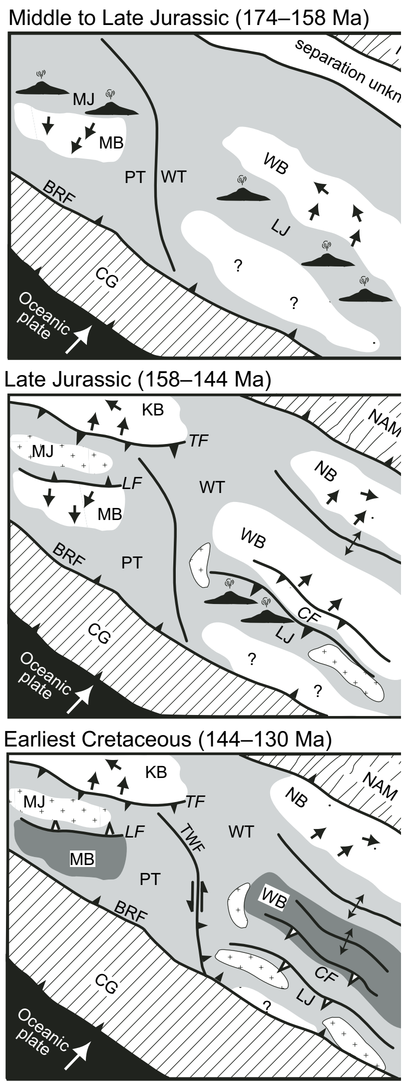

Figure 11. Sketch maps showing our preferred interpretation of the tectonic evolution of southern Alaska during late Mesozoic time. NAM—inboard terranes representing former continental margin of western North America. See Figure 1A for explanation of abbreviations and present distribution of sedimentary basins and tectonic features. This reconstruction includes restoration of ~130 km of Cretaceous-Tertiary dextral displacement along the Castle Mountain fault system (CCF in Fig. 1A) and ~40 km of latest Jurassic–Early Cretaceous sinistral displacement and overthrusting along the Taral–West Fork fault system (TWF in Figs. 1A and 11C). Paleolatitudes are not indicated given the lack of reliable constraints from the Wrangellia composite terrane. See text for discussion.

folded during latest Jurassic–earliest Cretaceous time. Renewed Cretaceous sediment accumulation may have been accommodated in part by thermal subsidence via reestablishment of arc magmatism along the inboard margin of the basin (EK in Fig. 1A) in combination with flexural subsidence along the outboard margin of the basin via thrusting along the Border Ranges fault (Pavlis et al., 1988) and/or expansion of the subduction complex (CG in Fig. 1A; Plafker et al., 1994). Middle Jurassic to Upper Cretaceous forearc basin strata were subsequently deformed by broad, open folds prior to strike-slip displacement along the Little Oshetna and Castle Mountain faults.

Regional Stratigraphic Relationships

The Naknek Formation is the most widespread Mesozoic formation exposed in the Peninsular terrane, occupying a 45-km-long outcrop belt in the southern Talkeetna Mountains (Jsu in Fig. 1B) and a ~1150-km-long outcrop belt along the Alaska Peninsula (PB in Fig. 1A). Previous stratigraphic analyses of the Naknek Formation focused on the Alaska Peninsula outcrop belt (Lankford and Magoon, 1978; Detterman and Reed, 1980; Detterman et al., 1996; Cucci et al., 1996; Wilson et al., 1999). Integration of our new data from the Talkeetna Mountains with published data from the Alaska Peninsula demonstrates regional similarities in the stratigraphy, provenance, and structural setting of the Naknek Formation, including: (1) northward-dipping reverse faults juxtaposing northernmost Naknek Formation outcrops with Middle Jurassic plutons; (2) a disconformity with topographic relief separating the Naknek Formation from underlying Middle Jurassic sedimentary strata; (3) Oxfordian deposition dominated by proximal conglomeratic mass-flow deposits and distal sandstone turbidites, mudstone, and *Buchia concentrica* fossils; (4) Kimmeridgian-Tithonian shelf deposition dominated by cross-stratified sandstone and *Buchia mosquensis* fossils; (5) mixed petrofacies with abundant felsic plutonic and mafic volcanic clasts; and (6) disconformable upper contact with Lower Cretaceous strata recording latest Jurassic–earliest Cretaceous depositional hiatus. Collectively, these observations demonstrate similar depositional histories for the Naknek Formation outcrops exposed in the Talkeetna Mountains and Alaska Peninsula.

Our new stratigraphic data from the Naknek Formation also provide improved constraints on the amalgamation history of the Wrangellia composite terrane. Stitching plutons demonstrate juxtaposition of the Wrangellia and Alexander terranes by middle Pennsylvanian time (Gardner et al., 1988), but unequivocal cross-cutting linkages between the Peninsular terrane and the adjacent Wrangellia terrane have not been reported. Upper Jurassic strata exposed within the Peninsular (Naknek Formation) and Wrangellia terranes (Kotsina Conglomerate, upper Root Glacier Formation) provide a regional stratigraphic linkage based on closely comparable depositional histories, including (1) deposition of conglomeratic marine mass-flow deposits that contain Oxfordian-Kimmeridgian mollusks; (2) a mixed petrofacies containing felsic plutonic clasts with Middle to Late Jurassic geochronologic ages; and (3) a regional disconformity with topographic relief that separates Middle and Upper Jurassic strata (Grantz, 1960a, 1960b; MacKevett, 1969, 1978; Trop et al., 2002; this study). These sedimentologic, compositional, and stratigraphic similarities suggest that the Peninsular terrane was joined with the combined Wrangellia-Alexander terrane by Late Jurassic time (Oxfordian-Kimmeridgian; 159–151 Ma). This stratigraphic linkage is compatible with the presence of early Late Jurassic (158–156 Ma) felsic intrusions within both the Peninsular and Wrangellia terranes in the Talkeetna Mountains (Snee et al., 2002; Rioux et al., 2002). Lithologically comparable Permian-Triassic strata are exposed in both the Peninsular and Wrangellia terranes, indicating a potentially longer shared history between the terranes (Plafker et al., 1989; Nokleberg et al., 1994).

Postdepositional Strike-Slip Displacement

At least two major episodes of strike-slip faulting prompted lateral displacement of Late Jurassic forearc basin deposits in the Wrangellia composite terrane. Displacement along the boundary between the Peninsular and Wrangellia terranes during the latest Jurassic–Early Cretaceous was characterized by overthrusting and ~40 km of sinistral strike-slip displacement along the Taral–West Fork fault system coeval with overthrusting along the Border Range fault (Fig. 1A; Plafker et al., 1989; Nokleberg et al., 1994). In the Wrangell Mountains region, this deformation event juxtaposed Late Jurassic plutons (LJ in Fig. 1A) against the Chugach accretionary prism, tectonically removed any Jurassic forearc basin deposits, and placed Jurassic forearc basin deposits of the Talkeetna Mountains (MB in Figs. 1A and 11) along strike with Jurassic retroarc basin deposits of the Wrangell Mountains (WB in Figs. 1A and 11). Jurassic forearc basin deposits of the Matanuska Valley–Talkeetna Mountains were subsequently displaced by strike-slip movement along the Castle Mountain fault (CCF in Fig. 1A). Late

Cretaceous to Tertiary piercing points record 20–40 km of dextral offset but do not constrain the timing of initial displacement (Grantz, 1966; Clardy, 1974; Detterman et al., 1976; Fuchs, 1980; Trop et al., 2003). The present outcrop distribution of the Naknek Formation, Jurassic plutons, and the Little Oshetna/Bruin Bay fault systems across the Castle Mountain fault provides a potential Jurassic piercing point for Late Jurassic–Early Cretaceous dextral displacement. Naknek Formation exposures in the Talkeetna Mountains and Alaska Peninsula record comparable depositional histories adjacent to coeval felsic plutons. The previously unmapped Little Oshetna fault (LF in Figs. 1A and 2) is comparable with the well-documented 480-km-long Bruin Bay fault (BF in Fig. 1A; Detterman and Reed, 1980) of the Alaska Peninsula (PB in Fig. 1A). Both faults strike northeast, dip northwest, exhibit reverse displacement, and juxtapose Middle to Upper Jurassic felsic plutons in the hanging wall against Middle to Upper Jurassic marine strata in the footwall. The Bruin Bay fault is truncated by the Castle Mountain fault ~10 km north of Beluga, Alaska, along Olson Creek based on outcrop data in combination with subsurface wells and seismic profiles (Magoon et al., 1976). Correlation of the Little Oshetna and Bruin Bay faults would require ~110–130 km of post–Late Jurassic dextral displacement along the Castle Mountain fault. Our inability to map the precise location of the intersection of the Little Oshetna and Castle Mountain faults (Fig. 1A) prevents a more precise displacement estimate. This proposed piercing point follows Hackett (1976), who proposed ~100 km of dextral displacement along the Castle Mountain fault based on offset Jurassic outcrop belts and geophysical anomalies attributable to Jurassic igneous rocks. Post-Jurassic offset of ~100–130 km along the Castle Mountain fault may reflect substantial Mesozoic displacement or indicate that the Cretaceous to Tertiary markers underestimate the total displacement along the fault.

Regional Tectonics and Basin Development

Late Jurassic exhumation and synorogenic sedimentation characterized forearc basins along the outboard (southern) segment of the Wrangellia composite terrane (PB, MB in Figs. 1A and 11) and retroarc basins along the inboard (northern) margin of the terrane (NB, KB, WB in Figs. 1A and 11; Manuszak and Ridgway, 2000; Trop et al., 2002; Ridgway et al., 2002; Eastham and Ridgway, 2002). Sedimentation began in each basin during Oxfordian to Kimmeridgian time based on age-diagnostic marine megafossils (Figs. 1A and 11; Richter, 1976; MacKevett, 1978; Imlay, 1981; Csejtey et al., 1992; Winkler, 1992). Measured stratigraphic sections from each basin document deposition mainly by submarine mass flows on unstable, high-gradient slopes influenced by basin-margin faults (CF, LF, BF in Figs. 1A and 11). Diagnostic clasts, paleocurrent indicators, lithofacies transitions, and detrital zircon ages from Upper Jurassic forearc basin deposits in the Talkeetna Mountains demonstrate outboard- (southward) directed sediment transport related to exhumation of Middle to Upper Jurassic felsic plutons that intrude the Peninsular terrane. Forearc exhumation and sedimentation overlapped with retroarc thrust-related sedimentation in the Wrangell Mountains basin and unroofing of the Wrangellia terrane and Upper Jurassic plutons (Chitina Valley batholith of MacKevett, 1978; Chitina arc of Plafker et al., 1989). Blind-thrust faults, source diagnostic clasts, and geochronologic ages of plutonic clasts (153 ± 1 Ma Ar-Ar age; 152 ± 6 Ma K-Ar age) in the Upper Jurassic Kotsina Conglomerate and Root Glacier Formation record syndepositional displacement and uplift along south-dipping thrust faults (Chitina thrust belt, CF in Figs. 1A and 11) located inboard of Upper Jurassic Chitina arc plutons (Grantz et al., 1966; Trop et al., 2002). Chitina arc plutons yield 153–150 Ma U-Pb zircon ages (Plafker et al., 1989; Roeske et al., 2003) and 146–138 Ma Ar-Ar and K-Ar ages (MacKevett, 1978; MacKevett et al., 1978; Winkler et al., 1980; Roeske et al., 1992, 2003).

Late Jurassic deformation and synorogenic sedimentation within the forearc basin and Chitina thrust belt were contemporaneous with subsidence and synorogenic sedimentation ~60–100 km further inboard (northward) of the Middle to Upper Jurassic plutons in the Nutzotin and Kahiltna basins. Conglomerate clast counts and sandstone compositional data from the Nutzotin and Kahiltna basins record exhumation of progressively deeper structural levels of the Wrangellia terrane during Late Jurassic–Early Cretaceous deposition (Manuszak, 2000; Eastham and Ridgway, 2002). In the Nutzotin basin, felsic plutonic clasts in conglomerate and 159–147 Ma U-Pb detrital zircon ages from sandstone document exhumation of Upper Jurassic plutons. Paleocurrent data demonstrate sediment flux away from the Wrangellia composite terrane in retroarc basins, including northward- to eastward-directed paleoflow in the Nutzotin basin and northward- to northwestward-directed paleoflow in the eastern Kahiltna basin. Upper Jurassic–Lower Cretaceous strata exposed along the inboard margin of the Alexander and Wrangellia terranes in southeastern Alaska (Gravina belt of Berg et al., 1972) record a similar erosional history. Clastic strata of the Gravina belt consist predominantly of marine sediment gravity flow deposits that were derived largely from Upper Jurassic arc source terranes, based on sandstone detrital modes (Cohen and Lundberg, 1993), granitic clasts with 158–154 Ma U-Pb zircon ages (Rubin and Saleeby, 1991), detrital zircons with 165–140 U-Pb ages (Kapp and Gehrels, 1998), and detrital biotites with 159–151 Ma Ar-Ar ages (Cohen et al., 1995).

We interpret Late Jurassic contractile deformation, pluton exhumation, and synorogenic sedimentation in retroarc and forearc basins as reflecting either initial accretion of the Wrangellia composite terrane to the margin of western North America or amalgamation of the Peninsular and Wrangellia terranes prior to final accretion. Late Jurassic accretion is indicated by the regional, crustal-scale nature of uplift and derivation of retroarc basin detritus from inboard terranes in the northern Kahiltna basin in south-central Alaska (Eastham and Ridgway, 2002) and the Gravina basin in southeastern Alaska (Gehrels et al., 1992; Kapp and Gehrels, 1998). According to this model, subsequent late Early to Late Cretaceous folding and structural imbrication of retroarc basin deposits in south-central Alaska (Richter, 1976; Csejtey et al., 1982; Nokleberg et al., 1985; Manuszak, 2000), Yukon Territory (Eisbacher, 1976), and southeastern Alaska (Rubin et al., 1990; Rubin and Saleeby, 1992; Gehrels et al., 1992; Haeussler, 1992; Haeussler et al., 1999) record postcollisional suturing of the terrane to the continental margin (e.g., Pavlis, 1982; McClelland et al., 1992; Gehrels, 2001; Ridgway et al., 2002; Trop et al., 2002). Alternatively, Late Jurassic–Early Cretaceous shortening and exhumation potentially reflect subduction-related deformation or initial juxtaposition of the Peninsular and Wrangellia terranes. The timing of Wrangellia-Peninsular amalgamation is loosely constrained by pre-Jurassic overlap assemblages (e.g., Nokleberg et al., 1994), and a detailed study of the terrane boundaries in the Talkeetna Mountains is necessary to resolve the Late Jurassic history of the two terranes. In interpreting the Naknek Formation as forming in a collisional forearc basin setting and the Kahiltna-Nutzotin-Gravina basins as forming in a collisional retroarc setting, a dual plate-subduction scenario is inferred (e.g., Monger et al., 1982; Rubin et al., 1990; Stanley et al., 1990), with subduction polarity of both plates dipping to the north (present coordinates), one beneath the Wrangellia composite terrane, and the other beneath the North America continental margin. Structurally emplaced ophiolite slivers exposed along the suture zone between the Wrangellia and Yukon composite terranes (Richter, 1976; Nokleberg et al., 1994) indicate the existence of a consumed oceanic plate. Moreover, the structural style of northeastward-dipping thrust faults and southwest-verging folds documented for the Nutzotin basin is consistent with a northward-dipping subduction zone between the Wrangellia composite terrane and North America (Richter, 1976; Manuszak, 2000).

From a broader perspective, structural and stratigraphic relations in southeast Alaska–British Columbia suggest initial collision of the Wrangellia composite terrane during the Middle Jurassic (e.g., McClelland and Gehrels, 1990; McClelland et al., 1992; Lewis et al., 1991; Thompson et al., 1991). Our data from south-central Alaska do not preclude Middle Jurassic collision, but evidence for regional deformation, exhumation, and synorogenic sedimentation is limited to Upper Jurassic and younger strata. Collectively, these regional relationships suggest diachronous accretion of the composite terrane (e.g., Pavlis, 1982, 1989), with the southeast Alaska–British Columbia segment colliding during Middle Jurassic time and the south-central Alaska segment colliding during Late Jurassic time, consistent with westward younging of retroarc basin deposits in southern Alaska (Fig. 1A; Wallace et al., 1989; Ridgway et al., 2002). Unfortunately, the paleolatitude of the composite terrane during initial collision and subsequent northward translation is loosely constrained (e.g., Cowan et al., 1997). Positioned ~12° north of the equator during Late Triassic time (Hillhouse and Coe, 1994), the south-central Alaska segment was translated northward to moderate paleolatitudes (near present-day Oregon) by latest Cretaceous time (Stamatakos et al., 2001) before its Eocene arrival at its present position (Hillhouse and Coe, 1994). Paleomagnetic analyses from Upper Jurassic–Lower Cretaceous strata, including the Naknek Formation (J. Stamatakos, 2003, personal commun.) and Gravina belt (Butler et al., 1997), did not yield reliable primary magnetizations.

CONCLUSIONS

1. New biostratigraphic and geochronologic data from the Naknek Formation constrain the timing of deposition of individual lithofacies associations. The lower 690 m of the Naknek Formation was deposited during early Oxfordian to early Kimmeridgian time. The upper 225 m of the Naknek Formation was deposited during early Kimmeridgian to early Tithonian time. These age data indicate that deposition of the coarse-grained lower Naknek Formation commenced contemporaneous with regional Late Jurassic crustal-scale shortening, pluton exhumation, and synorogenic sedimentation throughout the Wrangellia composite terrane.

2. Reconstruction of Naknek Formation depositional systems demonstrates that sedimentation was initially characterized by a high-gradient, southward-dipping basin floor during early Oxfordian to early Kimmeridgian time. Poorly sorted cobble-boulder conglomerate was deposited by submarine mass flows in proximal fan-delta environments. Gravelly mass flows transformed downslope into sandy turbidity currents on a channelized prodelta slope. During early Kimmeridgian–early Tithonian time, lower-gradient, shallow-marine shelf environments onlapped prodelta slope deposits prior to subaerial uplift of the basin floor.

3. Compositional data, U-Pb zircon ages of plutonic clasts, and southward-directed paleocurrent indicators from the Naknek Formation document Late Jurassic exhumation of Middle to Upper Jurassic plutons along the northern basin margin. Felsic plutonic clasts yield U-Pb zircon ages (167.6 ± 0.3 Ma; 166.5 ± 0.2 Ma, 164–159 Ma, 156.2 ± 0.2 Ma) that are equivalent to U-Pb zircon ages from petrographically similar felsic plutons exposed along the northern basin margin. The concentration of boulder-rich mass-flow deposits in the footwall of the northward-dipping Little Oshetna fault in combination with source-diagnostic clasts and geochronologic data is consistent with syndepositional displacement along the Little Oshetna fault. Steep depositional gradients prompted southward transport and deposition of poorly sorted gravel with abundant meter-size plutonic clasts and sand enriched in feldspar, hornblende, and pyroxene.

4. From a regional perspective, Late Jurassic synorogenic sedimentation and pluton exhumation in forearc basins along the outboard (southern) segment of the Wrangellia composite terrane were coeval with crustal-scale shortening and synorogenic sedimentation in retroarc basins along the inboard (northern) margin in the Kahiltna, Nutzotin, and Wrangell Mountains basins. Exhumation of Middle to Upper Jurassic plutons as well as deep structural levels of the Wrangellia and Peninsular terranes provided abundant coarse-grained clastic sediment along both the inboard and outboard margins of the composite terrane from south-central to southeastern Alaska. We interpret the regional nature of Late Jurassic crustal-scale deformation and synorogenic sedimentation as reflecting initial accretion of the composite terrane with the former continental margin of North America or amalgamation of the Wrangellia and Peninsular terranes prior to final accretion.

ACKNOWLEDGMENTS

This study was supported by the Forest Oil Corporation (to J.T.), Anschutz Corporation (to J.T.), Geological Society of America Undergraduate Research Fund (to D.Z.), and PricewaterhouseCoopers Undergraduate Research Fund (to D.Z.). Our analysis of the Naknek Formation would not have been possible without the original geologic mapping of the Talkeetna Mountains by Arthur Grantz. We are grateful to Michael Mickey and Stanley Kling for identifying foraminifera and radiolaria fossils, respectively. Members of the Talkeetna Arc project, including Peter Keleman, Jim Mattinson, Peter Clift, and Brad Hacker provided logistical support and useful discussions on the geology of the study area. Terry Pavlis and Bill McClelland provided thoughtful reviews that helped us improve the manuscript.

REFERENCES CITED

Barker, F., and Grantz, A., 1982, Talkeetna Formation in the southeastern Talkeetna Mountains, southern Alaska: An Early Jurassic andesitic intraoceanic island arc: Geological Society of America Abstracts with Programs, v. 14, no. 4, p. 147.

Barnes, F.F., 1962, Geologic map of lower Matanuska Valley, Alaska: U.S. Geological Survey Miscellaneous Investigations Map I-359, 1 sheet, scale 1:63,360.

Berg, H.C., Jones, D.L., and Richter, D.H., 1972, Gravina-Nutzotin belt—Significance of an upper Mesozoic sedimentary and volcanic sequence in southern and southeastern Alaska: U.S. Geological Survey Professional Paper 800-D, p. D1–D24.

Butler, R.F., Gehrels, G.E., and Bazard, D.R., 1997, Paleomagnetism of Paleozoic strata of the Alexander terrane, southeastern Alaska: Geological Society of America Bulletin, v. 109, p. 1372–1388, doi: 10.1130/0016-7606(1997)1092.3.CO;2.

Clardy, B.I., 1974, Origin of the lower and middle Tertiary Wishbone and Tsadaka Formations, Matanuska Valley, Alaska [M.S. thesis]: Fairbanks, Alaska, University of Alaska, 50 p.

Cohen, H.A., and Lundberg, N., 1993, Detrital record of the Gravina arc southeastern Alaska: Petrology and provenance of Seymore Canal sandstones: Geological Society of America Bulletin, v. 105, p. 1400–1414, doi: 10.1130/0016-7606(1993)1052.3.CO;2.

Cohen, H.A., Hall, C.M., and Lundberg, N., 1995, $^{40}Ar/^{39}Ar$ dating of detrital grains constrains the provenance and stratigraphy of the Gravina Belt, southeastern Alaska: Journal of Geology, v. 103, no. 3, p. 327–337.

Cole, R.B., 2003, Tertiary volcanism across the Wrangellia composite terrane of south-central Alaska: Geological Society of America Abstracts with Programs, v. 23, no. 6, p. 561.

Cowan, D.S., Brandon, M.T., and Garver, J.I., 1997, Geologic tests of hypotheses for large coastwise displacements—A critique illustrated by the Baja British Columbia controversy: American Journal of Science, v. 297, p. 117–173.

Crawford, M.L., Hollister, L.S., and Woodsworth, G.J., 1987, Crustal deformation and regional metamorphism across a terrane boundary, Coast plutonic complex, British Columbia: Tectonics, v. 6, p. 343–361.

Csejtey, B., Jr., Nelson, W.H., Jones, D.L., Silberling, N.J., Dean, R.M., Morris, M.S., Lanphere, M.A., Smith, J.G., and Silberman, M.L., 1978, Reconnaissance geologic map and geochronology, Talkeetna Mountains quadrangle, north part of Anchorage quadrangle, and southwestern corner of Healy quadrangle, Alaska: U.S. Geological Survey Open-File Report 78-558-A, 60 p., 1 sheet, scale 1:250,000.

Csejtey, B., Jr., Cox, D.P., Evarts, R.C., Stricker, G.D., and Foster, H.L., 1982, The Cenozoic Denali fault system and the Cretaceous accretionary development of southern Alaska: Journal of Geophysical Research, v. 87, p. 3741–3754.

Csejtey, B., Jr., Mullen, M.W., Cox, D.P., and Stricker, G.D., 1992, Geology and geochronology of the Healy quadrangle, south-central Alaska: U.S. Geological Survey, Miscellaneous Investigations Series Map I-1961, 3 sheets, scale 1:250,000.

Cucci, M.A., Morris, W.R., McGowen, J.H., Curry, R.P., Krueger, S.W., and Doherty, D.J., 1996, Depositional systems in a forearc basin; outcrop examples from the Upper Jurassic Naknek Formation of southern Alaska: Annual Meeting Abstracts—American Association of Petroleum Geologists and Society of Economic Paleontologists and Mineralogists, v. 5, p. 31.

Detterman, R.L., and Reed, B.L., 1980, Stratigraphy, structure, and economic geology of the Iliamna Quadrangle, Alaska: U.S. Geological Survey Bulletin 1368-B, 86 p.

Detterman, R.L., Plafker, G., Russell, G.T., and Hudson, T., 1976, Features along part of the Talkeetna segment of the Castle Mountain–Caribou fault system, Alaska: U.S. Geological Survey Miscellaneous Field Studies Map MF-738, scale 1:63,360.

Detterman, R.L., Case, J.E., Miller, J.W., Wilson, F.H., and Yount, M.E., 1996, Stratigraphic framework of the Alaska Peninsula: U.S. Geological Survey Bulletin 1969-A, 74 p.

Eastham, K.R., and Ridgway, K.D., 2002, Stratigraphy and provenance data from the Upper Jurassic to Upper Cretaceous Kahiltna assemblage of south-central Alaska, *in* Wilson, F.H., and Galloway, J.P., eds., Studies by the U.S. Geological Survey in Alaska, 2000: U.S. Geological Survey Professional Paper 1662, p. 45–53.

Eisbacher, G.H., 1976, Sedimentology of the Dezadeash flysch and its implications for strike-slip faulting along the Denali fault, Yukon Territory and Alaska: Canadian Journal of Earth Sciences, v. 13, p. 1495–1513.

Fuchs, W.A., 1980, Tertiary tectonic history of the Castle Mountain fault system in the Talkeetna Mountains [Ph.D. dissertation]: Salt Lake City, Utah, University of Utah, 152 p.

Gardner, M.C., Bergman, S.C., Cushing, G.W., MacKevett, E.M., Plafker, G., Campbell, R.B., Dodds, C.J., McClelland, W.C., and Mueller, P.A., 1988, Pennsylvanian pluton stitching of Wrangellia and the Alexander terrane, Wrangell Mountains, Alaska: Geology, v. 16, p. 967–971, doi: 10.1130/0091-7613(1988)0162.3.CO;2.

Gehrels, G.E., 2001, Geology of the Chatham Sound region, Southeast Alaska and coastal British Columbia: Canadian Journal of Earth Sciences, v. 38, p. 1579–1599, doi: 10.1139/cjes-38-11-1579.

Gehrels, G.E., McClelland, W.C., Samson, S.D., Patchett, J.P., and Orchard, M.J., 1992, Geology of the western flank of the Coast Mountains between Cape Fanshaw and Taku Inlet: Southeastern Alaska: Tectonics, v. 11, p. 567–585.

Gradstein, F.M., Agterberg, F.P., Ogg, J.G., Hardenbol, J., Van Veen, P., Thierry, J., and Huang, Z., 1994, A Triassic, Jurassic, and Cretaceous time scale, *in* Berggren, W.A., Kent, D.V., Aubry, M.P., and Hardenbol, J., eds., Geochronology, Time Scales, and Global Stratigraphic Correlation: SEPM, Special Publication 54, p. 95–125.

Grantz, A., 1960a, Geologic map of Talkeetna Mountains (A-2) quadrangle, Alaska and the contiguous area to the north and northwest: U.S. Geological Survey Miscellaneous Geologic Investigations Map I-313, 1 sheet, scale 1:48,000.

Grantz, A., 1960b, Geologic map of Talkeetna Mountains (A-1) quadrangle, Alaska and the south third of Talkeetna Mountains (B1) quadrangle, Alaska: U.S. Geological Survey Miscellaneous Geologic Investigations Map I-314, 1 sheet, scale 1:48,000.

Grantz, A., 1966, Strike-slip faults in Alaska: U.S. Geological Survey Open-File Report 66-53, 82 p.

Grantz, A., Thomas, H., Stern, T.W., and Sheffey, N.B., 1963, Potassium-argon and lead-alpha ages for stratigraphically bracketed plutonic rocks in the Talkeetna Mountains, Alaska, *in* Short Papers in Geology and Hydrology: U.S. Geological Survey Professional Paper 475-B, p. B56–B59.

Grantz, A., Jones, D.L., and Lanphere, M.A., 1966, Stratigraphy, paleontology, and isotopic ages of upper Mesozoic rocks in the southwestern Wrangell Mountains, Alaska: U.S. Geological Survey Professional Paper 550-C, p. 39–47.

Hackett, S.W., 1976, Speculative tectonic evolution of the Cenozoic Shelikoff Trough, south-central Alaska, *in* Short Notes on Alaskan Geology: Alaska Division of Geology and Geophysical Surveys Geologic Report 51, p. 13–17.

Haeussler, P.J., 1992, Structural evolution of an arc-basin: The Gravina belt in central southeastern Alaska: Tectonics, v. 11, p. 1245–1265.

Haeussler, P.J., Karl, S.M., Mortensen, J.K., Layer, P.W., and Himmelberg, G.R., 1999, Permian and Mid-Cretaceous deformation of the Alexander Terrane on Admiralty and Kupreanof Islands: Geological Society of America Abstracts with Programs, v. 31, no. 6, p. 60.

Haq, B.U., Hardenbol, J., and Vail, P.R., 1988, Mesozoic and Cenozoic chronostratigraphy and cycles of sea-level change, *in* Wilgus, C.K., et al., eds., Sea-level changes: An integration: Special Publication of the Society of Economic Paleontologists and Mineralogists, v. 42, p. 71–108.

Higgs, R., 1990, Sedimentology and tectonic implications of Cretaceous fan-delta conglomerates, Queen Charlotte Islands, Canada: Sedimentology, v. 37, p. 83–103.

Hillhouse, J.W., and Coe, R.S., 1994, Paleomagnetic data from Alaska: *in* Plafker, G., and Berg, H.C., eds., The Geology of Alaska: Boulder, Colorado, Geological Society of America, The Geology of North America, v. G-1, p. 797–812.

Imlay, R.W., 1981, Late Jurassic ammonites from Alaska: U.S. Geological Survey Professional Paper 1190, 40 p.

Imlay, R.W., and Detterman, R.L., 1973, Jurassic paleobiogeography of Alaska: U.S. Geological Survey Professional Paper 801, 34 p.

Jaffey, A., Flynn, K., Glendenin, L., Bentley, W., and Essling, A., 1971, Precision measurement of half-lives and specific activities of ^{235}U and ^{238}U: Physical Review C, v. 4, no. 5, p. 1889–1906.

Jones, D.L., 1964, Upper Cretaceous (Campanian and Maestrichtian) ammonites from southern Alaska: U.S. Geological Survey Professional Paper 432, 53 p.

Jones, D.L., 1967, Cretaceous ammonites from the lower part of the Matanuska Formation, southern Alaska, with a stratigraphic summary by Arthur Grantz: U.S. Geological Survey Professional Paper 547, 49 p.

Kapp, P.A., and Gehrels, G.E., 1998, Detrital zircon constraints on the tectonic evolution of the Gravina belt, southeastern Alaska: Canadian Journal of Earth Sciences, v. 35, p. 253–268, doi: 10.1139/cjes-35-3-253.

Kidwell, S.M., 1991, The stratigraphy of shell concentrations, *in* Allison, P.B., and Briggs, D.E.G., eds., Taphonomy: Releasing the Data Locked in the Fossil Record: New York, Plenum Press, p. 211–290.

Krogh, T.E., 1973, A low contamination method for the hydrothermal decomposition of zircon and extraction of U and Pb for isotopic age determinations: Geochimica et Cosmochimica Acta, v. 37, p. 485–494, doi: 10.1016/0016-7037(73)90213-5.

Lankford, S.M., and Magoon, L.B., 1978, Petrography of the Upper Jurassic through Oligocene sandstones in the Cape Douglas–Kamishak Hills area, lower Cook Inlet: Geological Survey Circular, v. 295, p. B60–B62.

Lewis, P.D., Haggart, J.W., Anderson, R.G., Hickson, C.J., Thompson, R.I., Dietrich, J.R., and Rohr, K.M.M., 1991, Triassic to Neogene evolution of the Queen Charlotte region: Canadian Journal of Earth Sciences, v. 28, p. 854–869.

Lowe, D.R., 1982, Sedimentary gravity flows II: Depositional models with special reference to the deposits of high-density turbidity currents: Journal of Sedimentary Petrology, v. 52, p. 279–297.

Ludwig, K.R., 1999, User's Manual for Isoplot/Ex, Version 2.01: A Geochronological Toolkit for Microsoft Excel: Berkeley, Berkeley Geochronology Center Special Publication 1a, 47 p.

MacKevett, E.M., Jr., 1969, Three newly named Jurassic formations in the McCarthy C-5 quadrangle, Alaska: U.S. Geological Survey Bulletin 1274-A, p. A37–A49.

MacKevett, E.M., Jr., 1978, Geologic map of the McCarthy quadrangle, Alaska: U.S. Geological Survey Miscellaneous Investigation Series Map I-1032, 1 sheet, scale 1:250,000.

MacKevett, E.M., Jr., Smith, J.G., Jones, D.L., and Winkler, G.R., 1978, Geologic map of the McCarthy C-8 quadrangle: U.S. Geological Survey Geologic Quadrangle Map GQ-1418, 1 sheet, scale 1:63,360.

Magoon, L.B., Adkison, W.L., and Egbert, R.M., 1976, Map showing geology, wildcat wells, Tertiary plant fossil localities, K-Ar age dates, and petroleum operations, Cook Inlet area, Alaska: U.S. Geological Survey Miscellaneous Investigations Series Map I-1019, scale 1:250,000.

Manuszak, J.D., 2000, Sedimentary and structural record of Late Jurassic–Early Cretaceous collisional tectonics, Nutzotin and Mentasta Mountains, east-central Alaska [M.S. thesis]: West Lafayette, Indiana, Purdue University, 291 p.

Manuszak, J.D., and Ridgway, K.D., 2000, Stratigraphic architecture of the Nutzotin Mountains sequence, Nutzotin and Mentasta Mountains, Alaska, *in* Pinney, D.S., and Davis, P.K., eds., Short notes on Alaskan geology 1999: Fairbanks, Alaska, Division of Geological and Geophysical Surveys Professional Report 119, p. 63–75.

Mattinson, J.M., 1987, U-Pb ages of zircons: A basic examination of error propagation: Chemical Geology, v. 66, p. 151–162.

Mattinson, J.M., 2001a, Partial dissolution analysis (PDA) of zircon: Past, present, future: Roanoke, Virginia, Eleventh Annual V.M. Goldschmidt Conference, Abstract 3368.

Mattinson, J.M., 2001b, Multi-step high-resolution Pb/U and Pb/Pb zircon age spectra: Combined annealing, partial dissolution, and TIMS analysis: Eos (Transactions American Geophysical Union), v. 82, Fall Meeting Supplement, Abstract V22C–1056.

Mattinson, J.M., 2003, CA (Chemical Abrasion)-TIMS: High-resolution U-Pb zircon geochronology combining high-temperature annealing of radiation damage and multi-step partial dissolution analysis: Eos (Transactions American Geophysical Union), v. 84, Fall Meeting Supplement, Abstract V22E–06.

McClelland, W.C., and Gehrels, G.E., 1990, The Duncan Canal shear zone: A right-lateral shear zone of Jurassic age along the inboard margin of the Alexander terrane: Geological Society of America Bulletin, v. 102, p. 1378–1392, doi: 10.1130/0016-7606(1990)1022.3.CO;2.

McClelland, W.C., Gehrels, G.E., and Saleeby, J.B., 1992, Upper Jurassic–Lower Cretaceous basinal strata along the Cordilleran margin: Implications for the accretionary history of the Alexander-Wrangellia-Peninsular terrane: Tectonics, v. 11, p. 823–835.

Miller, J.W., and Detterman, R.L., 1985, The *Buchia* zones in Upper Jurassic rocks on the Alaska Peninsula: Geological Survey Circular, v. 945, p. 51–53.

Monger, J.W.H., Price, R.A., and Templeman-Kluit, D.J., 1982, Tectonic accretion and the origin of the two major metamorphic and plutonic welts in the Canadian Cordillera: Geology, v. 10, p. 70–75.

Nemec, W., 1990, Aspects of sediment movement on steep delta slopes: Coarse-grained deltas: International Association of Sedimentologists Special Publication 10, p. 29–73.

Nemec, W., and Steel, R.J., 1984, Alluvial and coastal conglomerates: Their significant features and some comments on gravelly mass-flow deposits, *in* Koster, E.H., and Steel, R.J., eds., Sedimentology of Gravels and Conglomerates: Canadian Society of Petroleum Geologists Memoir, v. 10, p. 1–31.

Nokleberg, W.J., Jones, D.L., and Silberling, N.J., 1985, Origin and tectonic evolution of the Maclaren and Wrangellia terranes, eastern Alaska Range, Alaska: Geological Society of America Bulletin, v. 9, p. 1251–1270.

Nokleberg, W.J., Plafker, G., and Wilson, F.H., 1994, Geology of south-central Alaska, *in* Plafker, G., and Berg, H.C., eds., The Geology of Alaska: Boulder, Colorado, Geological Survey of America, The Geology of North America, v. G-1, p. 311–365.

Pavlis, T.L., 1982, Origin and age of the Border Ranges fault of southern Alaska and its bearing on the late Mesozoic tectonic evolution of Alaska: Tectonics, v. 1, p. 343–368.

Pavlis, T.L., 1989, Middle Cretaceous orogenesis in the northern Cordillera: A Mediterranean analog of collision-related extensional tectonics: Geology, v. 17, p. 947–950, doi: 10.1130/0091-7613(1989)0172.3.CO;2.

Pavlis, T.L., Monteverde, D.H., Bowman, J.R., Rubenstone, J.L., and Reason, M.D., 1988, Early Cretaceous near-trench plutonism in southern Alaska: A tonalite-trodhjemite intrusive complex injected during ductile

thrusting along the Border Ranges fault system: Tectonics, v. 7, p. 1179–1199.
Pickering, K.T., Stow, D.A.V., Watson, M., and Hiscott, R.N., 1986, Deep-water facies, processes, and models: A review and classification scheme for modern and ancient sediments: Earth-Science Review, v. 23, p. 75–174, doi: 10.1016/0012-8252(86)90001-2.
Plafker, G., and Berg, H.C., 1994, Overview of the geology and tectonic evolution of Alaska, *in* Plafker, G., and Berg, H.G., eds., The Geology of Alaska: Geological Society of America: Boulder, Colorado, The Geology of North America, v. G-1, p. 989–1021.
Plafker, G., Nokleberg, W.J., and Lull, J.S., 1989, Bedrock geology and tectonic evolution of the Wrangellia, Peninsular, and Chugach terranes along the Trans-Alaskan Crustal Transect in the northern Chugach Mountains and southern Copper River basin, Alaska: Journal of Geophysical Research, v. 94, p. 4255–4295.
Plafker, G., Moore, J.C., and Winkler, G.R., 1994, Geology of the southern Alaska margin, *in* Plafker, G., and Berg, H.G., eds., The Geology of Alaska: Boulder, Colorado, Geological Society of America, The Geology of North America, v. G-1, p. 389–450.
Postma, G., 1990, Depositional architecture and facies of river and fan deltas, a synthesis, *in* Colella, A., and Prior, D.B., eds., Coarse-grained deltas, International Association of Sedimentologists Special Publication 10, p. 13–27.
Richter, D.H., 1976, Geologic map of the Nabesna quadrangle, Alaska: U.S. Geological Survey, Miscellaneous Geological Investigations Series Map I-932, 1 sheet, scale 1:250,000.
Ridgway, K.D., Trop, J.M., Nokleberg, W.J., Davidson, C.M., and Eastham, K.D., 2002, Mesozoic and Cenozoic tectonics of the eastern and central Alaska Range: Progressive basin development and deformation within a suture zone: Geological Society of America Bulletin, v. 114, p. 1480–1504, doi: 10.1130/0016-7606(2002)1142.0.CO;2.
Rioux, M.R., Mattinson, J.M., Hacker, B.R., and Grove, M., 2002, Growth and evolution of the accreted Talkeetna arc, south-central Alaska: Solutions to the "arc paradox": Eos (Transactions American Geophysical Union), v. 83, Fall Meeting Supplement, Abstract V12C-11.
Rioux, M., Hacker, B., Mattinson, J., Kelemen, P., Hanghoj, K., and Plank, T., 2003, The role of intermediate to felsic plutonism in the accreted Talkeetna arc, south-central Alaska: Geological Society of America Abstracts with Programs, v. 35, no. 6, p. 430, Abstract 174-15.
Roeske, S.M., Mattinson, J.M., and Armstrong, R.L., 1989, Isotopic ages of glaucophane schists on the Kodiak Islands, southern Alaska, and their implications for the Mesozoic tectonic history of the Border Ranges fault system: Geological Society of America Bulletin, v. 101, no. 8, p. 1021–1037, doi: 10.1130/0016-7606(1989)1012.3.CO;2.
Roeske, S.M., Pavlis, T.L., Snee, L.W., and Sisson, V.B., 1992, $^{40}Ar/^{39}Ar$ isotopic ages from the combined Wrangellia-Alexander terrane along the Border Ranges fault system in the eastern Chugach Mountains and Glacier Bay, Alaska, *in* Bradley, D.C., and Ford, A.B., eds., Geologic Studies in Alaska by the U.S. Geological Survey, 1990: U.S. Geological Survey Bulletin 1999, p. 180–195.
Roeske, S.M., Snee, L.W., and Pavlis, T.L., 2003, Dextral-slip reactivation of an arc-forearc boundary during Late Cretaceous–early Eocene oblique convergence in the northern Cordillera, *in* Sisson, V.B., Roeske, S.M., and Pavlis, T.L., eds., Geology of a transpressional orogen developed during ridge-trench interaction along the north Pacific margin: Geological Society of America Special Paper 371, p. 141–169.
Rubin, C.M., and Saleeby, J.B., 1991, The Gravina Sequence: Remnants of a mid-Mesozoic oceanic arc in southern southeast Alaska: Journal of Geophysical Research, v. 96, p. 14,551–14,568.
Rubin, C.M., and Saleeby, J.B., 1992, Tectonic history of the eastern edge of the Alexander terrane, southeastern Alaska: Tectonics, v. 11, p. 586–602.
Rubin, C.M., Saleeby, J.B., Cowan, D.S., Brandon, M.T., and McGroder, M.F., 1990, Regionally extensive mid-Cretaceous west-vergent thrust system in the northwestern Cordillera, implications for continent-margin tectonism: Geology, v. 18, p. 276–280, doi: 10.1130/0091-7613(1990)0182.3.CO;2.
Snee, L.W., Schmidt, J.M., Oswald, P.J., and Prueher, E.M., 2002, Jurassic to early Tertiary plutonic suites of the northern Talkeetna Mountains, Alaska: Geological Society of America Abstracts with Programs, v. 34, no. 5, p. 100.
Sohn, Y.K., Kim, S.B., Hwang, J.G., Bahk, J.J., Choe, M.Y., and Chough, S.K., 1997, Characteristics and depositional processes of large-scale gravelly Gilbert-type foresets in the Miocene Doumsan fan delta, Pohang basin: Journal of Sedimentary Research, v. 67, p. 130–141.
Stamatakos, J.A., Trop, J.M., and Ridgway, K.D., 2001, Late Cretaceous paleogeography of Wrangellia: Paleomagnetism of the MacColl Ridge Formation, southern Alaska, revisited: Geology, v. 29, p. 947–950, doi: 10.1130/0091-7613(2001)0292.0.CO;2.
Stanley, W., Labson, V., Nokleberg, W., Csejtey, B., and Fisher, M., 1990, The Denali fault system and Alaska Range of Alaska: Evidence for underplated Mesozoic flysch from magnetotelluric surveys: Geological Society of America Bulletin, v. 102, p. 160–173, doi: 10.1130/0016-7606(1990)1022.3.CO;2.
Stow, D.A.V., and Piper, D.J.W., 1984, Deep-water fine-grained sediments: Facies models, *in* Stow, D.A.V., and Piper, D.J.W., eds., Fine-grained sediments: Deep-water processes and facies: Geological Society [London] Special Publication 15, p. 611–646.
Stow, D.A.V., Bishop, C.D., and Mills, S.J., 1982, Sedimentology of the Brae oilfield, North Sea: Fan models and controls: Journal of Petroleum Geology, v. 5, p. 129–148.
Surlyk, F., 1984, Fan-delta to submarine fan conglomerate of the Volgian-Valanginian Wollaston Forland Group, East Greenland, *in* Koster, E.H., and Steel, R.J., eds., Sedimentology of Gravels and Conglomerates: Canadian Society of Petroleum Geologists Memoir 10, p. 359–382.
Szuch, D.A., 2002, Synorgenic sedimentation along the arcward margin of a Mesozoic forearc basin, Naknek Formation, Talkeetna Mountains, Alaska [B.S. thesis]: Lewisburg, Pennsylvania, Bucknell University, 260 p.
Thompson, R.J., Haggart, J.W., and Lewis, P.D., 1991, Late Triassic through early Tertiary evolution of the Queen Charlotte basin, British Columbia, with a perspective on hydrocarbon potential, *in* Woodsworth, G.J., ed., Evolution and hydrocarbon potential of the Queen Charlotte basin, British Columbia: Geological Survey of Canada Paper 90-10, p. 3–29.
Trop, J.M., Ridgway, K.D., Manuszak, J.D., and Layer, P.W., 2002, Sedimentary basin development on the allochthonous Wrangellia composite terrane, Mesozoic Wrangell Mountains basin, Alaska: A long-term record of terrane migration and arc construction: Geological Society of America Bulletin, v. 114, p. 693–717, doi: 10.1130/0016-7606(2002)1142.0.CO;2.
Trop, J.M., Ridgway, K.D., and Spell, T.L., 2003, Synorogenic sedimentation and forearc basin development along a transpressional plate boundary, Matanuska Valley–Talkeetna Mountains, southern Alaska, *in* Sisson, V.B., Roeske, S., and Pavlis, T.L., eds., Geology of a transpressional orogen developed during ridge-trench interaction along the north Pacific margin: Geological Society of America Special Paper 371, p. 89–118.
van der Heyden, P., 1992, A Middle Jurassic to early Tertiary Andean-Sierran arc model for the Coast Belt of British Columbia: Tectonics, v. 11, p. 82–97.
Wallace, W.K., Hanks, C.L., and Rogers, J.F., 1989, The southern Kahiltna terrane: Implications for the tectonic evolution of southwestern Alaska: Geological Society of America Bulletin, v. 101, p. 1389–1407, doi: 10.1130/0016-7606(1989)1012.3.CO;2.
Wilson, F.H., Dover, J.H., Bradley, D.C., Weber, F.R., Bundtzen, T.K., and Haeussler, P.J., 1998, Geologic map of central (interior) Alaska: U.S. Geological Survey Open-File Report 98-133-A, 63 p.
Wilson, F.H., Detterman, R.L., and DuBois, G.D., 1999, Digital data for the geologic framework of the Alaska Peninsula, southwest Alaska, and the Alaska Peninsula Terrane: U.S. Geological Survey Open-File Report 99-317, 41 p, http://wrgis.wr.usgs.gov/open-file/of99-317/.
Winkler, G.R., 1992, Geologic map and summary geochronology of the Anchorage 1° × 3° quadrangle, southern Alaska: U.S. Geological Survey Miscellaneous Investigations Series Map I-2283, 1:250,000 scale.
Winkler, G.R., Silbermann, M.L., Grantz, A., Miller, R.J., and MacKevett, E.M., Jr., 1980, Geologic map and summary geochronology of the Valdez quadrangle, southern Alaska: U.S. Geological Survey Open-File Report 80-892-A, 1 sheet, scale 1:250,000.

Manuscript Received by the Society 24 January 2004
Revised Manuscript Received 30 June 2004
Manuscript Accepted 10 September 2004

Printed in the USA